Diploma Thesis

Expansion phenomena during internal sulfate attacks (ISA)

Submitted in satisfaction of the requirements for the degree

of Diplom-Ingenieur

Of the TU Wien, Faculty of Civil Engineering

_____

Diplomarbeit

Treiberscheinungen im inneren Sulfatangriff

Ausgeführt zum Zweck der Erlangung des akademischen Grades eines

Diplom-Ingenieurs

Eingereicht an der technischen Universität Wien, Fakultät für Bauingenieurwesen

Von

Hossam Al Daffaie Bsc.

Matr.Nr.: 1622510

Unter der Anleitung von

Ass.Prof.Dr. **Teresa Liberto**

Dipl.- Ing. Dr.techn. **Johannes Kirnbauer**

Univ.- Prof. PhD **Agathe Robisson**

Institut für Werkstofftechnologie, Bauphysik und Bauökologie

Forschungsbereich Baustofflehre, Werkstofftechnologie

Technische Universität Wien

Lilienthalgasse 14, 1030 Wien, Österreich

Wien, im Oktober 2022   _____

Abstract

The durability of concrete is governed by many factors, such as climate conditions, cement chemical composition, and the mechanical properties of the concrete mixture. Sulfate attack (SA) is a phenomenon that strongly affect the durability of concrete after several years, which make studying SA very challenging. If the sulfate ions are internally available in the concrete formulation for example using recycled concrete contaminated with gypsum, the attack is called internal sulfate attack (ISA). The knowledge on ISA is limited and the issues linked to expansive behavior lack proper characterization. In this work, we investigated the influence on ISA of key design variables such as: water to cement ratio w/c, cement type, cement hydration state, moisture and temperature variation, gypsum content and fineness. We used several methods to measure the ISA-induced expansion, such as: prism length variation, Le-Chatelier expansion rings (LC), and oedometer-cell integrated in a compression device. Rheological tests were also conducted to monitor the early hydration of pastes linked to the formation of secondary ettringite.

The rheological tests showed that the early reactivity of hydrated cement Fondu was very sensitive to the addition of hydrated gypsum (HG). In blended cement (Blaue + Fondu), the HG addition fragilized the paste probably due to delayed hydration of C_3S and C_2S. The hydrated cement Blaue and the blended hydrated cement (Blaue + Fondu) showed high expansion in modified (confined expansion) LC tests. The confinement in LC was effective when measuring cement pastes with high consistency and high expansion values. The oedometer device was very sensitive to temperature changes, which made the measurement of the crystallization pressure with this device very difficult. Mortar prisms with fresh cement powders with HG addition showed initial small expansion followed by shrinkage after each weathering cycle.

Kurzfassung

Die Dauerhaftigkeit von Beton hängt von vielen Faktoren ab, wie den klimatischen Bedingungen, der chemischen Zusammensetzung des Zements und den mechanischen Eigenschaften der Betonmischung. Sulfatangriff (SA) ist ein Phänomen, das die Dauerhaftigkeit von Beton nach mehreren Jahren stark beeinträchtigt, was die Untersuchung von SA sehr schwierig macht. Wenn die Sulfat-Ionen im Inneren der Betonrezeptur vorhanden sind, z. B. bei Verwendung von mit Gips kontaminiertem Recyclingbeton, wird der Angriff als interner Sulfatangriff (ISA) bezeichnet. Das Wissen über ISA ist begrenzt, und die mit dem expansiven Verhalten verbundenen Probleme sind nicht ausreichend charakterisiert. In dieser Arbeit untersuchten wir den Einfluss wichtiger Variablen wie Wasser-Zement-Verhältnis (w/z), Zementart, Zementhydratationszustand, Feuchtigkeits- und Temperatursänderungen, Gipsgehalt und Gipsfeinheit auf ISA. Zur Messung der ISA-induzierten Ausdehnung wurden verschiedene Methoden angewandt, wie z. B.: Prismenlängenänderung, Le-Chatelier-Ausdehnungsringe (LC) und eine in eine Druckvorrichtung integrierte Ödometerzelle. Außerdem wurden rheologische Tests durchgeführt, um die primäre Hydratation des Zementleims in Verbindung mit der Bildung von sekundärem Ettringit zu untersuchen.

Die rheologischen Tests zeigten, dass die frühe Reaktivität des hydratisierten Zements Fondu sehr empfindlich auf die Zugabe von hydratisiertem Gips (HG) reagiert hat. Bei der Zementmischung (Blaue + Fondu) führte die Zugabe von HG zu einer Schwächung des Zementsteins, was wahrscheinlich auf eine verzögerte Hydratation von C_3S und C_2S zurückzuführen ist. Der hydratisierte Zement Blaue und die Zementmischung (Blaue + Fondu) zeigten eine hohe Ausdehnung im modifizierten LC-Test (zweidimensionale bzw. eingeschränkte Ausdehnung). Der eingeschränkte LC-Test war für die Messung der Ausdehnung vom Zementleim mit hoher Konsistenz und hohen Ausdehnungswerten effektiv. Das Ödometergerät war sehr empfindlich gegenüber Temperaturänderungen, was die Messung des Kristallisationsdrucks mit diesem Gerät sehr schwierig gemacht hat. Mörtelprismen mit frischen Zementpulvern mit HG-Zusatz zeigten anfangs eine geringe Ausdehnung. Die Werte der Ausdehnung wurden nach jedem Verwitterungszyklus reduziert.

Acknowledgement

I would like to express my sincere thanks and deep sense of gratitude to my supervisor Univ. Prof. Agathe Robisson PhD, Chief of the research department Building Material and Technology, for her valuable guidance, esteem discussion and continuous encouragement.

I wish to extend my gratitude and heartful appreciation to my co-supervisors Assistant. Prof. Dr. Teresa Liberto and Dipl. Ing. Dr. techn. Johannes Kirnbauer for their valuable guidance, esteem suggestions, and support throughout this thesis.

I wish to express my sincere thanks to Dr. Maurizio Bellotto for his valuable discussion and advice, and Prof. Maria Chiara Dalconi for implementing the XRPD tests.

Sincere thanks to laboratory engineer Andreas Hausenberger for his greatly appreciated help in the setups and the calibration of the oedometer tests. Furthermore, I would like to thank laboratory engineer Benjamin Marksteiner sincerely for his help in different tests and preparations. My thanks are extended to my collogues in the laboratory for their valuable discussions.

I would like to thank my girlfriend Christine for her love, support, and encouragement.

I would like to thank my parent, my sisters and brothers for their continuous love, patience, and support. To my family who gave me everything, I present them this work as a gift and as a sign of my utmost gratitude.

Table of Contents

List of figures

List of tables

1. Introduction

Durability of concrete is governed by many factors, such as climate conditions, cement chemical composition, and the mechanical properties of the concrete mixture. Sulfate attack (SA) is a phenomenon that strongly affects the durability of concrete in the long run (10s of years) [2]. SA can cause concrete deterioration such as cracking or spalling [3] and mechanical properties loss [4]. Severe structural damages can occur when a concrete structure is exposed to high amounts of sulfate (severe structural damages in foundations near salt lakes in west China are noticed) [5]. In general, concrete resistance to SA is governed by many interdependent factors [6] such as:

- cement type (aluminum or C_3A content) and particle size distribution of the cement powder (PSD);
- water to cement ratio (w/c) in the cement slurry or in concrete;
- temperature (curing, storage, and hydration temperature) and moisture gradient due to external weather (e.g., cooling and rain in winter vs. heating and drying in summer)
- exposure to sulfate: both concentration of sulfate and the type of the sulfate (magnesium, calcium, or sodium sulfate) affect the mechanism of deterioration.

If the source of sulfate ions is external, we can talk about external sulfate attacks (ESA). Internal sulfate attacks (ISA), instead, happen when the source of sulfate is inside the concrete, as for example when recycled concrete aggregate used in the mixture is contaminated with gypsum. In this case, all the necessary conditions for the formation of swelling products are already present within the cement, so deterioration may occur more quickly [7].

Actions implemented to mitigate ESA in concrete are: (a) reducing w/c to lower the concrete permeability, (b) using C_3A-free cement or cement with a minimum aluminate content, (c) improving concrete compaction, and (d) surface finishing to minimize sulfate ions diffusion into the concrete [6, 8]. In the case of ISA, a denser compaction of the concrete and lower porosity is disadvantageous to resist the crystallization pressure exerted via ettringite formation [7, 9, 10]. ISA in recycled concrete has been less studied, and the issues linked to expansive behavior lack proper characterization. This lack of data is considered a limitation in the reutilization of building demolition wastes. An expansive behavior due to ISA can also cause deterioration and loss in mechanical properties in very dense concretes such as ultra-high-performance one (UHPC) [11].

The so-called physical sulfate attack (PSA) consists of cycles of crystallization and decomposition of sulfate salt crystals and/or ettringite in the pore structure of concrete or cement paste [6], leading to a fatigue-induced degradation [12, 13]. If, for example, the sodium sulfate is the attacking medium, the cycles of dissolution and precipitation of salts inside the concrete will lead to phenomena such as efflorescence and subflorescence. In structures near the sea or near a source rich in sulfate, the salt enters the pores of the permeable concrete. If the water evaporates, the concentration of the salts increases to the degree of supersaturation, and it recrystallizes inside the concrete pores. The crystallization pressure exerted on the concrete might then reach and exceed the tensile strength of the concrete, generating cracks [14, 15]. PSA, generated through solubilization and recrystallisation of salts once they enter the concrete (through permeability), is therefore a function of change in temperature and humidity inside the concrete.

The chemical sulfate attack (CSA), on the other hand, is due to chemical reactions between the cement clinker phases (C_3A) or cement hydration products (e.g., calcium hydroxide and monosulfate) with the sulfate ions. These chemical reactions lead to the formation of products like ettringite or gypsum, and under certain conditions (and after significant amount of time) to expansion and deterioration of the concrete. The chemical reactions and the formation of these swelling products begin with the mixing of cement with water. They continue over the concrete lifetime upon diffusion of sulfates into the concrete from external sources (e.g., soil or groundwater) or upon internal sources of contamination with gypsum (e.g., using recycling

concrete contaminated with gypsum). The deterioration of the concrete (e.g., cracking or loss of strength) happens only under certain conditions (e.g., formation of secondary ettringite in substantially hardened concrete, when the ettringite recrystallizes in small nanometric pores). The chemical reactions can be called "attack" only if they are accompanied by degradation of the concrete or loss in mechanical properties [6, 15].

One of the evidences on the correlation between the amount of ettringite formed and the resulting expansion is shrinkage compensation cement. Using a blended cement made of aluminum rich cement (like calcium aluminum cement), normal Portland cement and gypsum leads to additional expansion due to extra ettringite formation. The shrinkage caused by water evaporation, water diffusion to the soil or chemical and autogenous shrinkage will be compensated by the expansion resulted from ettringite formation [16, 17].

In both PSA and CSA, the ettringite forms following the chemistry explained in the next section.

1.1 Chemistry of sulfate attack

The chemical reactions leading to the formation of gypsum, monosulfate and ettringite once the cement is in contact with water (i.e., fresh paste, reactions 1-3) and later in time (hardened state, reactions 4-5) are explained below [18-20]:
Cement chemical notation are used to describe the cement constituent for the reactions below:

$CS2H = CaSO_4 . 2\,H_2O$ = gypsum
$C_3A.3CS.32H = 3CaO.Al_2O_3.3Ca.SO_4.32H_2O$= ettringite
$C_3A.CS.12H$ = calcium aluminate monosulfate hydrate
$C_3A = 3CaO.Al_2O_3$= tricalcium aluminate
$CS = CaSO_4$
$H = H_2O$

$$CH = Ca(OH)_2$$
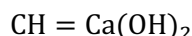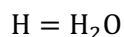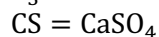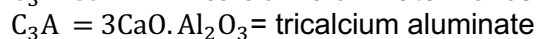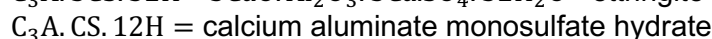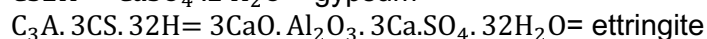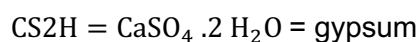
In (1) gypsum $CS2H$ is formed upon reaction of sulfate ions (SO_4^{2-}) with calcium cations (Ca^{2+}). The effect of gypsum formation on expansion is still not clear in literature [6].

$$Ca^{2+} + SO_4^{2-} + 2H \rightarrow CS2H + 2(OH)^- \qquad (1)$$
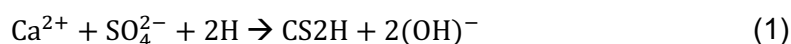
In (2), the gypsum reacts with the unhydrated C_3A to form early (or primary) ettringite. The time frame for primary ettringite formation is the first 24 hours. Within this time, the cement paste is still deformable (not hardened). The formation of this primary ettringite is hence not considered harmful and leads to no expansion [21-23].

$$C_3A + 3\,CS2H + 26\,H \rightarrow C_3A.3CS.32H \quad (\Delta v = 0\ \%) \qquad (2)$$
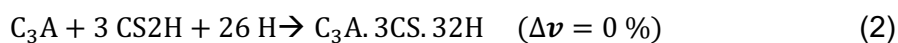
Upon lack of gypsum, the early ettringite reacts with the remaining unhydrated C_3A to form monosulfate, following equation (3). This phase is unstable and can transform again in (secondary) ettringite when sulfate and calcium ions become available, following equation (4). The associated volumetric change is $2.48 \cdot 10^{-4}\ \frac{m^3}{mol}$, i.e. 1 mol of ettringite resulting from this equation will cause a voluminous expansion= $2.48 \cdot 10^{-4}\ m^3$ [19].

$$C_3A.3CS.32H + 2C_3A + 4H \rightarrow C_3A.CS.12H \qquad (3)$$

$$C_3A.CS.12H + 2CH + 20H + 2SO_4^{2-} \rightarrow \mathbf{C_3A.3CS.32H} + 4(OH)^- \qquad (4)$$
$$(\Delta v = 2.48 \cdot 10^{-4}\ \frac{m^3}{mol})$$
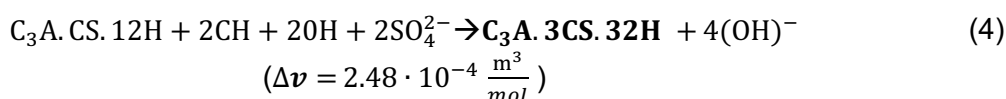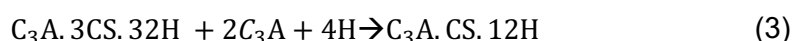
Secondary ettringite can also form by the reaction of the remaining unreactive C_3A with the calcium hydroxide (hydration product from C_3S), water and sulfate ions, following (5). This reaction is giving expansion as specified by Δv [19], meaning that 1 mol of ettringite resulting from this equation will cause a voluminous expansion= $3.94 \cdot 10^{-4} \ m^3$

$$C_3A + 3CH + 26H + 3SO_4^{2-} \rightarrow \mathbf{C_3A.\,3CS.\,32H} \quad (\Delta v = 3.94 \cdot 10^{-4} \ \tfrac{m^3}{mol}) \qquad (5)$$
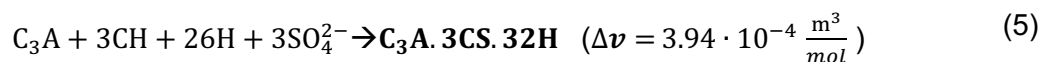
Overall, the transformation of 1 mol of C_3A ($\rho = 3.04 \ \tfrac{g}{cm^3}$) into 1 mol of ettringite ($\rho = 1.75 \ \tfrac{g}{cm^3}$) is accompanied roughly by 8-fold increase in volume [18].

The formation of secondary ettringite (reactions 4 and 5) happens in substantially hardened concrete. The expansion is therefore harmful and might lead under certain conditions to deterioration and cracking of the cement paste or concrete. This delayed ettringite formation may happen after several months to several years of casting [23, 24]. The molar ratio of $CS2H/C_3A$ controls which hydration products (ettringite, monosulfate) will form [19].[1]

1.2   Role of sulfate

Gypsum is added to cement clinker in small amount (i.e., 5% by wt. of cement) during the milling or after its production [25]. The purpose of addition of gypsum is to increase the specific surface area of cement during the milling process (i.e., the cement contains more fine particles because the gypsum is easier to mill than the cement clinker) and to prevent the flash setting of the clinker phase C_3A upon contact with water. The sulfate is added in form of calcium sulfate or alkali sulfate (sodium or potassium sulfate) or combination of both of them. If C_3A reacts as a pure phase alone with water (i.e., in absence of a sulfate source), the hydration products will be C_2AH_8 and C_4AH_{13} or C_4AH_{19}. These are unstable phases and eventually will transform to the more stable hydrogarnet phase C_3AH_6. These intermediate products are responsible for the flash setting, which strongly reduces the available time for placement and compaction of concrete. Moreover, the cement phases cannot complete their hydration process due to the fast hardening. If the sulfate is available, the hydration product will be instead primary ettringite ($C_3A.\,3CS.\,32H$). The primary ettringite covers the C_3A particles with a barrier of ettringite layer, preventing the further hydration of C_3A with water. In this way, enough workability of the concrete is available [19, 26, 27].

Increasing the gypsum content in the cement (e.g., internal contamination) or bringing sulfate ions from groundwater or soil into the concrete may lead to the formation of additional secondary ettringite and eventually to expansion. The higher the gypsum quantity, the more severe the expansion, as shown by Odler and Gasser: for added gypsum of 0.9, 10 and 15% the measured linear expansion in cement pastes made of the susceptible clinker was 5 %, 40% and 175% respectively [17, 28].

The severity of sulfate attacks for different sulfate contents is shown in table 1. According to this table, the severity is categorized into moderate, severe, and very severe exposure based on the amount of the SO_4 soluble in soil or in groundwater. The concrete must be designed based on this sulfate exposure to have a specific w/c ratio, minimum compressive strength, minimum amount of supplementary cementitious material and minimum air content [14].

---

[1] The formation of ettringite or monosulfate depends on the molar ratio of $CS2H/C_3A$. If the molar ratio= 1, then only monosulfate form. If it is=3 then only ettringite will form. Between 1-3 molar ratio, both monosulfate and ettringite will form.

Degree of Exposure	Water-Soluble Sulfate (SO$_4$) in Soil (%)	Sulfate (SO$_4$) in Groundwater (mg/L)	Minimum 56-Day Compressive Strength (MPa)	Maximum Water/Binder Ratio	Air Content Category	Cementing Materials to Be Used
Moderate	0.10–0.20	150–1,500	30	0.50	2[a]	20E[b], 40[c] or 50E[d]
Severe	0.20–2.0	1,500–10,000	32	0.45	2[a]	50t
Very severe	Over 2.0	Over 10,000	35	0.40	2[a]	50t

[a]Air category 2 requires air contents of 5%–8% for 10 mm maximum size of aggregate, 4%–7% for 14–20 mm aggregate and 3%–6% for 28–40 mm aggregate.
[b]Type 20E cement is similar to an ASTM Type II (moderate heat of hydration) cement; the E indicates that this is a blended cement.
[c]Type 40 cement is equivalent to an ASTM Type IV (low heat of hydration) cement.
[d]Type 50E cement is similar to an ASTM Type V (high sulfate resistance) cement; the E indicated that this is a blended cement.
   Modified from CSA Standard A23.1.

Table 1 Severity of sulfate attack and the requirement of concrete based on the exposure condition [14](adapted from the Canadian standard A23.1)

1.3 Role of Temperature

Concrete can be subjected to high temperatures during hydration and curing. For example, precast concrete may be steamed or heat cured at 60-70 °C to raise the initial compressive strength and to enable demolding of the concrete or the prestressing at early ages [29]. Temperature increase can also occur when large amounts of concrete are poured, due to heat of hydration, reaching temperature above 70°C. At this temperature, the water in the concrete will partially evaporate, leading to the increase of the total porosity of the concrete. This can also cause an incomplete concrete hydration because there is less water available for the cement phases to hydrate. The strength of the concrete will then decrease because of both the increased porosity and the low-rate of concrete hydration. The concrete under these conditions can be subject to deterioration more easily and cracks can develop on the surface [30]. The sulfate can diffuse more easily into concrete with more cracks (increase in permeability).

Raising the curing temperature of concrete above 70°C will lead to the dissolution of ettringite formed at the beginning of the hydration. The subsequent storage in water (20°C) will lead to recrystallisation of ettringite. This delayed secondary ettringite formation in the confined pores (few nanometers) of concrete is the reason for the beginning of its deterioration. The ratio of SO_3/Al_2O_3 above 0.5 is a condition in which the delayed formation of ettringite is encouraged [14, 15, 17, 23].

Lower temperatures (10-20°C), on the other hand, can lead to the formation of thaumasite (calcium sulfosilicate, $CaSiO_3 . CaCO_3 . CaSO_4 . 15H_2O$) which is responsible for another type of sulfate attack, and lead to the decomposition of calcium silicate hydrates (C-S-H). It causes softening of the concrete and loss in strength. It is necessary that both calcium sulfate and a source of carbonate ions are available together for thaumasite to form. The carbonate sources come either from concrete exposure to the air and the subsequent carbonation phenomenon, or from cement containing limestone added during the production or milling of the cement [7, 14, 31, 32].

1.4 Studies on sulfate attack

As already mentioned, the formation of the secondary ettringite, which degrades the concrete structure, can happen after several months to several years (4-40 years) after casting [2, 23, 24].

 Most of the studies on sulfate attack aim to accelerate the formation of delayed (or secondary) ettringite and the deterioration process. One of the methods used for the acceleration is exposing the concrete to solutions with high concentrations of sulfate. The time for the sulfate to penetrate into the concrete via diffusion is a function of the cement or concrete permeability. Once the sulfate reached into the core of the concrete, a chemical reaction between the sulfate and the hydration products occurs, delayed ettringite forms, subsequently expansion develops over time and the concrete cracks. The other method used is to expose concrete or cement

paste samples to weathering cycles of drying and wetting, or cooling and heating, to simulate the effect of temperature and humidity level changes on the deterioration. In the wetting cycles, the samples are either partially or completely submerged in water (as a reference sample) or in solution with elevated sulfate concentration and with ambient temperature (about 20°C). This stage is then followed by drying cycle at elevated temperature (e.g., 40°C) [33-36].

Xie and coworkers [37] have exposed concrete samples to drying / wetting cycles and to various concentrations of sodium sulfate solution (0, 5% by weight). The investigated samples were either fully or partially immersed in sulfate solution (23°C) for 3 days. The temperature of the drying cycles was 45°C for about 4 days. These cycles lasted for 40 weeks. It was found that the concrete fully submerged showed the least deterioration because only chemical attack happens under this exposure. The concrete subject to drying wetting cycles showed the highest deterioration, especially under partial submersion conditions. The combination of both chemical and physical sulfate attack on the same time is the reason for the higher grade of deterioration.

In another study from Wang and coworkers [13], the drying / wetting cycles effect on the deterioration of concrete was also studied. It is argued that by this kind of exposure, the sulfate ions enter the concrete by means of capillary forces in addition to normal diffusion and penetration (as when the concrete is fully submerged in solution). The wetting cycles allow a higher quantity of sulfate ions to penetrate the concrete, which promotes the precipitation of hydration products in the concrete pores, leading to an increase in strength. The drying process causes the supersaturation of the solution and precipitation of the salt crystals. These crystals, in return, exert pressure on the pore walls, driving expansion and subsequent deterioration. The drying / wetting cycles ultimately cause the concrete to fail due to cyclic fatigue (initial filling effect during wetting and expansion due to salt crystallization during drying).

Other experimental works [33-36] that combine both weathering cycles (physical sulfate attack) and exposure to high concentrations of sulfate (chemical sulfate attack), ranged between 6 months to 1 or 2 years. They focus on accelerating the damage by increasing the concrete permeability (by means of physical attack). The changes in the microstructure of the cement, the elastic modulus of elasticity, quantification of the hydration products (by means of XRD), expansion and weight change are all parameters included in the investigation methods.

One of the longest studies on the sulfate attack phenomenon lasted for 40 years. This study was implemented by the American bureau of reclamation in 1940. The effect of w/c ratio, addition of pozzolanic material and the C_3A and C_3S content of the cement were explored.

Based on the review of Monteiro and coworkers [2] on these long tests, the w/c ratio played a major role in the failure of investigated samples. The samples with w/c ratio less than 0.45 did not show failure (with the failure defined when expansion is greater than 0.5%) until the end of testing time (40 years) regardless of the C_3A content. This means that these samples have very low permeability and therefore only minimal or no sulfate diffusion occurs, and therefore no expansion. The second most important factor which controls the expansion or the failure is the amount of C_3A in cement. When the C_3A and w/c increase, the expansion happens much earlier (in the fourth year for w/c~0.475 and C_3A above 6% and high content of C_3S). An increased amount of C_3S accelerates the deterioration as well because the mechanism for the deterioration will be not only ettringite and gypsum formation but also C-S-H decomposition. Even with C_3A-free cements, the concrete deteriorated in less than 25 years, due to a different mechanism. The cements with high C_3S content suffer softening upon SA (probably due to delayed C_3S hydration). They develop less strength and become therefore less resistant to expansion resulting from the reaction of C_4AF with the sulfate. In all these samples, regardless of the influence of the single factors, and the measures to mitigate the expansion, the samples start to show length expansion (and failure) after a significant amount of time (at least four years).

1.5 Methodology

One of the most popular methods to study the sulfate attack is measuring the expansion in intervals after increasing periods of time. Prisms of cement mortar or concrete are made and the change in length is measured to obtain the expansion in time [31]. The change in weight over time can indicate also the formation of new hydration products leading to increase in weight [7]. The loss in weight on the other hand indicates deterioration for example by scaling or leaching.

Other tests in combination with expansion measurements are:
- compressive strength and modulus of elasticity evolution over time [38];
- scanning electron microscopy (SEM) to study the evolution of the microstructure during the time of sulfate attack;
- X-ray diffraction (XRD) to quantify the crystalline hydration products;
- calorimetry tests to follow up the evolution of reaction heat linked with the formation of new hydration products;
- standard chemical titration to quantify the sulfate concentration;
- X-ray spectroscopy to relate the change in microstructure observed by SEM to the products causing the damage [4];
- plasma spectrometry to measure the leaching of cations (e.g., calcium ions) in the storage solutions [39];
- energy dispersive spectroscopy to measure the molar ratio of the products investigated by means of SEM. Based on the molar ratio and by comparison to the molar ratio of known crystals, the existence of ettringite or gypsum can be confirmed [8];
- Mercury intrusion porosimetry to investigate the pore structure after sulfate attacks [8, 13, 37];
- ultrasonic waves to measure the change in dynamic modulus of elasticity when drying wetting cycles are involved [8].

1.6 Motivation of the study & methodology

Using recycling concrete in the building industry is a matter of important economic and ecological interest. The natural resources for cement production are limited, and the continuous cement production is consuming these resources. Moreover, the CO_2 release during the cement production is one of the major sources of contamination leading to the climate change. The recycling of concrete waste and its use in the construction industry is already practiced and aims to achieve ecological and economic benefits [37, 40].

The complexity of the SA physical chemistry led to a large amount of research so far, mostly focused on ESA, which sometimes present contradictory results and controversial interpretations [6]. The ISA is less explored than ESA and requires further studies to understand its deterioration mechanisms. The expansion due to the ISA phenomenon is especially relevant when recycled concrete is used. The concrete wastes contain cement hydrated to a substantial degree. This hydrated cement might have several compositions that affect or endanger the durability as a result of ISA. The original amount of C_3A, the aluminum content, the ettringite and AFm phases and original gypsum or sulfate content are all factors of impact on the structural safety and durability. Hydrated gypsum or additional amount of sulfate are also found in the concrete wastes. They originate for example from the plastering work or due to diffusion from soil or groundwater into the core of concrete [37, 41].

In this thesis, cement hydration state (fresh and hydrated), water/cement ratio (w/c), fineness and concentration of gypsum, and drying and wetting cycles were the investigation parameters to study ISA.

Different hydrated cements (with different chemical compositions) were produced to study the ISA. These hydrated cements once milled, were then mixed with hydrated gypsum to encourage the formation of (secondary) ettringite (during the new hydration process, once mixed with water) and to accelerate the expansion. This process is meant to mimic the

excessive expansion that occurs when utilizing recycled concrete. The results can also be helpful to identify the cement types that cause the most damage.

The methods used in this study are a combination of both traditional and novel tests. Prisms and Le Chatelier rings were involved in this study to investigate the expansion during weathering cycles of water submersion and drying. Oscillatory rheological tests were used to estimate the early reactivity of hydrated cements and the evolution of the cohesivity and deformability of these cements with an increasing amount of HG addition. Then, an oedometer cell integrated in compressing device was also used to measure the stress resulting from the secondary ettringite formation in a confined space with drying wetting cycles. All of these methods aim to link the deterioration of different cement types (upon internal contamination with hydrated gypsum) with the secondary ettringite formation. As already mentioned, the severity of sulfate attack is maximized in this investigation. The hydrated gypsum is added directly into the (hydrated and fresh) cements during the investigation, eliminating the necessity of sulfate diffusion into the concrete and thus reducing the time necessary for the deterioration to happen [7]. The cyclic heating and drying encourage the fast cyclic dissolution and reprecipitation of the expansive products inside the cement pastes [9, 33].

1.6.1 Prism

Generally, mortar prisms are produced by mixing sand, aggregate, water and cement according to the norm [42]. After mixing, the cement mortar is placed and compacted into steel formwork to obtain standard dimensions prisms (40 x 40 x 160 cm). To measure the expansion of the prisms over time, metal pins are placed inside the steel formwork. The prisms are let set for one day then the steel formwork is dismantled.

The initial length of the prisms is measured. To investigate the expansion due to sulfate attacks, the prisms are normally placed in container with a solution of high sulfate concentration to simulate the external sulfate attack (ESA). The change in length is measured periodically and the expansion of the prisms is plotted with time.

In this thesis, the internal sulfate attack (ISA) was investigated and simulated by replacing part of the fresh cement powder with hydrated gypsum (HG). Parameters affecting the expansion of the prisms were varied to test their effect on the resulting expansion. These parameters were: 2 w/c ratios (0.5 and 0.65), 3 concentrations of HG (0, 5 and 10%), fineness of HG (fine HG=1 mm and coarse HG=1-4 mm). The physical sulfate attack was additionally simulated by exposing the prisms to drying wetting cycles to accelerate the expansion and to mimic realistic exposure of the concrete to the weather (drying and heating in summer and wetting and cooling in winter).

1.6.2 Rheology:

 The science that studies the flow and deformation of liquid or soft matters is called rheology (Mezger 2015).

The rheometer is the device used for studying the behavior of the viscoelastic material under a certain deformation. The deformations (i.e., shear) applied by the rheometer to a material could be rotational or oscillatory. Oscillatory rheological tests on dense suspensions (i.e., gel, paste) are used to measure their properties at rest (i.e., elastic regime), as sketched in the figure 1 [43].
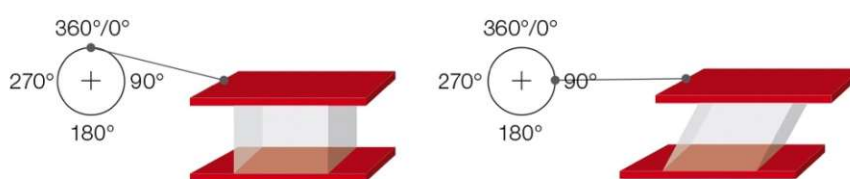

Figure 1 Two plates model to describe the oscillatory test
(Mezger, 2015)

In this figure, a material is placed between the two plates of a stress-controlled rheometer. In this case, the bottom plate is fixed, and the upper plate moves right and left with a certain amplitude stress (or deformation) imposed by the rotor. The movement of the plate at a constant speed result in oscillation with constant frequency. The rheometer imposes an amplitude strain γ (or stress) and measure and amplitude shear stress τ (or strain), as shown in figure 2 [1].
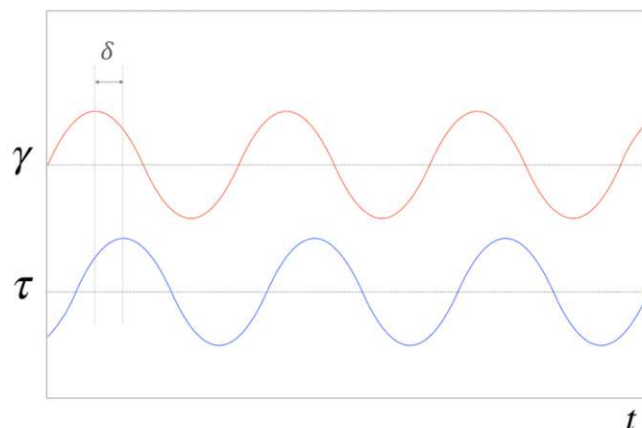

Figure 2 Deformation γ imposed to a viscoelastic material
and the response of the material τ.
The curves are out of phase with a phase lag δ (Liberto, 2018)

If the stress and strain are in phase ($\delta = 0$), we have a purely elastic material, when the phase lag is equal to $\delta = \pi/2$, we have instead a purely viscous material. Dense suspensions are mainly viscoelastic, showing an intermediate behaviour ($0 < \delta < \pi/2$).

The viscous and the elastic response of a viscoelastic material are characterised by G' (storage modulus) and G'' (loss modulus). G' and G'' are calculated according to the following equations [1]:

$$G' = \frac{\tau 0}{\gamma 0} \cos(\delta) \qquad (1)$$

$$G'' = \frac{\tau 0}{\gamma 0} \sin(\delta) \qquad (2)$$

The storage modulus G' is linked to the ability of the sample to restore its original condition after the applied deformation is removed. If the sample does not restore its original status after removal of the applied deformation, then some of the applied energy is lost due to motion and the internal friction between the molecules (the energy is dissipated as heat) and this is expressed by G''. Depending on the suspension type these moduli can be frequency dependent [1].

Small amplitude sweep oscillatory tests (or small amplitude oscillatory shear SAOS) are used to study the deformation of a material without destroying the structure and it can be applied either as strain sweep (shear-strain) or as stress sweep (shear-stress). The frequency is kept fixed and the amplitude deformation (or strain) is increased gradually. The linear viscoelastic region (LVE) is obtained by the amplitude sweep and it represents the range in which the structure of the material is not destroyed during the test (i.e., G' and G'' in the linear regime), as described in the material and methods section [43].

The time-dependant viscoelastic behaviour of the material is studied by fixing both the strain (or stress) amplitude (measured by SAOS in the LVE regime) and the frequency in test intervals. The results are plotted as evolution of G' and G'' with time [43].

To study the early reactivity of hydrated cement slurries, we apply 3 intervals. A short time structuration as preparatory step, an amplitude sweep to characterise the LVE region of the

pastes, and a long-time structuration to study the material evolution at rest without destroying the structure, as detailed in the next chapter.

1.6.3 Le Chatelier ring

The Le Chatelier expansion rings (LC) is a test method developed in EN-196-3 to examine the soundness of cements in the presence of free lime. The LC ring (the ring =30 mm in diameter and the needle indicators= 150 mm in length) is made of a curved thin sheet of corrosion resistant metal and needles. The ring can open with negligible force and will not resist the expansion of cement. Fresh cement paste with standard consistency is placed inside the ring. The paste is then left for 1 day to hydrate. The sample with the ring will then be placed in boiling water bath. The difference in distance between the needles is recorded (after one day and after the water bath). If the distance exceeds a specific value, then the cement expansion is considered unacceptable. No confinement is applied in this test and the cement paste and the needles are free to expand [44].

In this study, the expansion of the cement paste was measured by applying confinement to the LC rings. The LC rings were confined in the vertical direction and allowed expansion only in the diagonal direction. Figure 3 shows the LC rings with the confinement system.
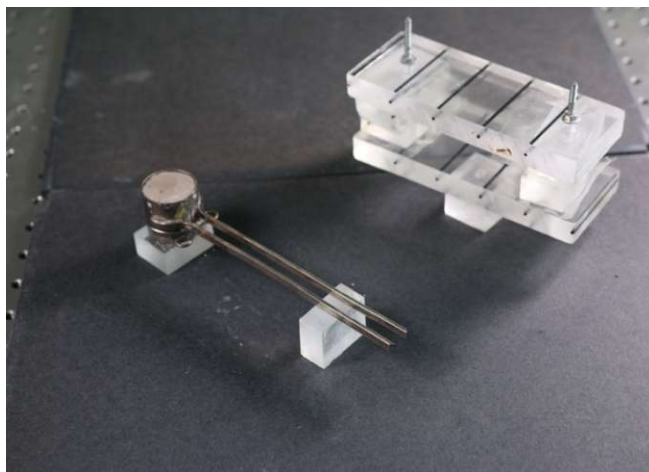
Figure 3 LC expansion rings with the confinement

The confining system was made of upper and lower plates of Plexiglas. The gap width between the plates = 31.5 mm.

1.6.4 Oedometer:

The standard oedometer test is developed to study the one-dimensional compression or swelling and for characterizing the strain- stress behavior in soil samples [45]. When a sample of soil is restrained to expand in diagonal direction and a steady load is applied to it, the pore water pressure will increase, and the water eventually will drain outside the soil and the volume of the soil will decrease (consolidate). The displacement accompanies this shrinkage in volume is recorded under full saturation of the soil sample with water. The properties of soil during this test are studied by different criteria: how much pressure can the soil withstand before it consolidates, the compressibility of the soil with respect to the void content and the ability of the soil to be recompressed after consolidation [46].

The sample is placed inside a thick steel ring (oedometer) to apply confinement and to allow one dimensional expansion in the direction perpendicular to the ring. Two automatic test modes can be selected:
 (a) strain-controlled test mode: a constant strain is applied to the sample or the sample will be hold in fix position. If the sample swells, the resulting swelling pressure (stress) will be automatically measured and plotted with time via load sensor;

(b) stress-controlled mode, a constant stress is applied into the sample and the resulting strain (shrinkage or swelling) of the sample will be measured via deformation sensor.

The sample is loaded via the compression device integrated into the system (maximum load of 10 kN). Water is continuously added to the sample from one side of the oedometer and discharged from the other side to keep the sample under full saturation.

The oedometer was used in this study to quantify the crystallization pressure resulting from ettringite formation upon internal contamination of the cement samples with hydrated gypsum. The ettringite formation is expansive and the volume of the sample should therefore increase. The consequent swelling apply internal pressure inside the cement samples. Because the samples were confined in diagonal direction, only a vertical expansion was possible. The stress resulting from this expansion was recorded automatically via the load sensor, and stress evolution was plotted with time. Figure 4 shows the oedometer integrated in a compressing device (WILLE GEOTECHNIK CO.)
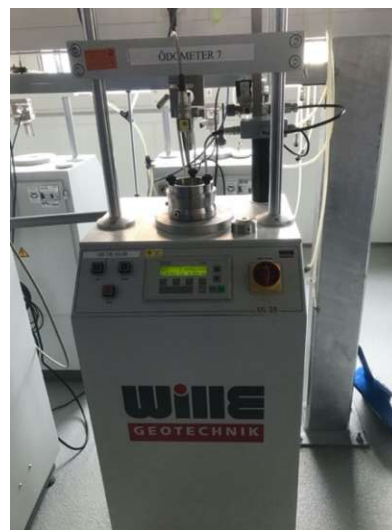

Figure 4 Oedometer integrated in compression device

2. Material and methods

2.1 Material

To simulate the internal sulfate attack, three different cement types were chosen: aluminum-rich cement (Fondu), ordinary Portland cement (Der Blaue) and sulfate resistant cement (C_3A-free, Der Contragress).

Cement Fondu (from Lafarge company) is a calcium aluminate cement, which is rich in aluminate phases (> 40%). It can be used either alone as the main cement for structural construction purposes or can be combined with other cements to produce material with special properties. For example, cement Fondu can be used in combination with ordinary Portland cement (OPC) to make a blended cement, which can be used for construction purposes like tile adhesive, or as fast repair material for roads. The hydration products of such blended cement are ettringite, AFm phases, calcium hydroxide CH, calcium silicate hydrate C-S-H and aluminum hydroxide AH_3. Rapid hardening, rapid drying, rapid setting and shrinkage compensation are the properties of this blend [16].

Ordinary Portland cement (Der Blaue) is the most common used cement in building industry. The main clinker phases of this cement are C_3S, C_2S, C_3A, C_4AF. The C_3S is responsible for the strength gain through the hydration with water and then precipitation of C-S-H and Portlandite (CH). The C_2S is also responsible for slow strength gain of the cement paste. Gypsum is already present in cement and it is added in small amount (~5%) to avoid the fast reaction of C_3A once in contact with water causing a loss of workability, as already mentioned in the intro. This cement has a low resistance to sulfate attack, which is why it should not be used in places with high contamination levels with sulfate [26, 47].

Sulfate resistant cement (Der Contragress) does not contain C_3A but only C_4AF, which dissolves and reacts more slowly [48, 49]. If it is attacked with sulfate, no ettringite is expected to form, unless the cement contains impurities during the production. For this reason, no expansion is expected to happen in this cement due to the lack of reactive aluminate (C_3A). This cement is therefore considered as highly resistant to sulfate attack and can be used in places rich with sulfate. It can be used in foundation construction, even if the soil is categorized as highly aggressive.

These cements were used either fresh or hydrated in presence of an excess of gypsum. In case of prisms length change measurements, fresh cements were used with hydrated gypsum (HG). In case of all other tests (rheology, LC expansion rings and oedometer), hydrated cements (with HG) were used.

2.1.1 Hydrated cement production and characterization

To simulate recycled concrete and accelerate ISA, hydrated cement powders were produced. Fresh cement powders were weighted using an electro scale (up to 0.5 g weighing accuracy). The cement then was placed in the bowl of electronic mixer. The necessary amount of water was weighted in the same way and added carefully afterward to the cement powder. Figure 5 shows the electronic mixer used for the mixing process.

Figure 5 Mortar Mixer

The automatic mixing program was used. The cement slurry was mixed slowly for 1 minute. The mixing was stopped briefly to homogenously mix the cement with the water using a spatula. Then the automatic fast mixing program was chosen and lasted for extra 3 minutes. The w/c ratios used were: 0.5 for Der Blaue and Der Contragress cement pastes and 0.3 for the Fondu one.

No chemical additives were used (e.g., superplasticizer or water reducing agents). Air entrainments and cement replacement with pozzolanic materials were also avoided here. Normal tap water was used in all the tests (except in rheology tests distilled water was used). These simplifications are useful in studying the phenomenon of sulfate attack to avoid any further influences on the response of the investigated cements.

The cement pastes were then casted in steel prisms (40 x 40 x 160 cm) and let set for 1 day. The prisms were covered with plastic sheets to prevent water evaporation. Figure 6 shows the casted prisms.

Figure 6 Cement paste casting to prepare the hydrated cements

The prisms were demolded after 1 day and kept in a climate chamber for one month to hydrate. The temperature in this room was 22 ± 2 °C and the relative humidity was 63 ± 5 %. To guarantee the maximum possible amount of hydration, the prisms were placed over a grid in a box partially filled with water. The relative humidity in this way was raised to 100%. After the hydration, the prisms were then heated to 60°C in the oven for two days. The heating process helped drying the prisms to easily break them in the next step. The temperature during the drying was kept at 60°C to avoid destabilization of the ettringite formed already during the hydration process. The prisms were then crushed into smaller size in a jaw crusher to make the milling process easier. The crushed hydrated cements were placed in ceramic balls miller (Erich Bolling GmbH&Co) to grind the cement into fine particles. The milling machine is shown in figure 7.
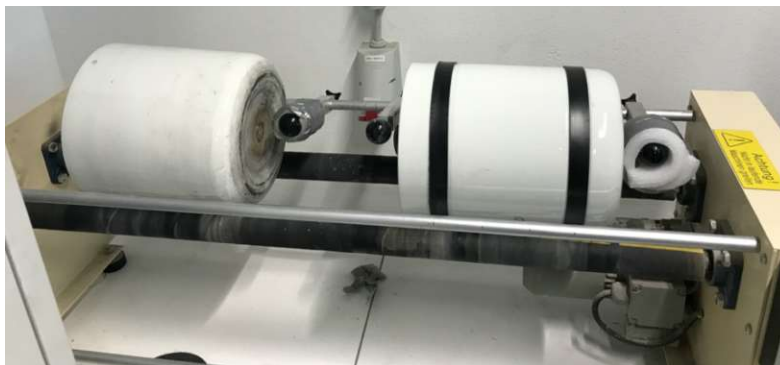
Figure 7 Ceramic balls miller

The milling was optimized by changing the diameter and the number of the used ceramic balls to get the smallest particle size possible of the hydrated cements. Figure 8 shows the milled cement powder and the ceramic balls used.

Figure 8 The result of the milling and the ceramic balls

After the milling process, all cements were sieved to a dimension lower than 1 mm. These hydrated cements were used as a simulation of recycled cements and called HF (hydrated fondu), HB (hydrated Blaue) and HC (hydrated Contragress).

The particle size distribution (PSD) of the milled hydrated cements is plotted in figure 9. Master sizer 3000 from the company Malvern Pananalytical was used for the particle size distribution analysis by laser diffraction.

Figure 9 Particle size distribution of the milled cement

The x-axis shows the particle size of the hydrated cements after the milling process and the y-axis shows the volume density (%). I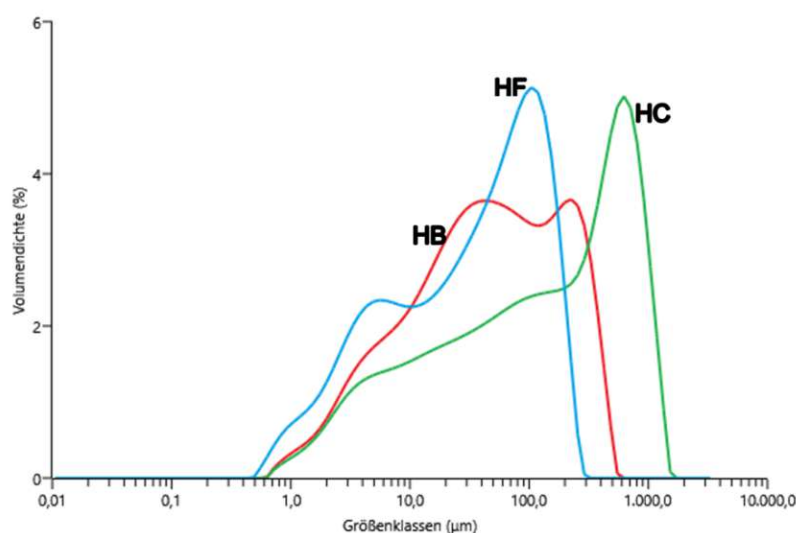t can be seen from the PSD that HF has the finest particles after milling, HC has the coarsest particles, this explain the difference in water addition to obtain a paste with the same consistency as discussed later. The values of D10, D50 and D90 are reported in table 2.

Sample name	Dx (10) (μm)	Dx (50) (μm)	Dx (90) (μm)
HB (hydrated Blaue)	4.70	44.90	258.00
HC (hydrated Contragress)	5.52	139.00	794.00
HF (hydrated Fondu)	2.96	36.60	145.00

Table 2 Particle size distribution of the milled cement (D10, D50 and D90)

Fresh industrial gypsum (company Knauf) was mixed with water (w/gypsum =0.67) and let hydrate for 1 month. The hydrated gypsum (HG) was also dried in oven (60°C) for two days. It was then broken and sieved. The hydrated gypsum (HG) was then sieved and sorted in two categories (size <1 mm and size 1-4 mm). It was used to contaminate the cements internally. The addition of HG is varied each time (0%, 5%, 10% and 25% HG) and the response of the material in different tests was investigated. This way the severity of sulfate attack was simulated. The 0% HG represents no sulfate attack and the addition of 25% HG represents the most severe sulfate attack investigated in this thesis.

X-ray powder diffraction (XRPD) on the hydrated cements powder (before the addition of hydrated gypsum HG) and on the HG was conducted in the lab of Padua University (Italy). The phases of the hydrated cements are quantified and listed in the tables below (Tables 3-6).

In table 3, it is seen that the industrial hydrated gypsum content on gypsum is only 72%. It contains amongst other impurities like dolomite (12%), and calcite (5%). The amount of sulfate in gypsum is equal to 45% [50]. This means that adding 5, 10 and 25% hydrated gypsum will cause additional amount of sulfate (additional to the amount of sulfate content originally available in the cements used) equals to 1.62% (severe exposure), 3.24% and 8.1% (very severe exposure) respectively (see table 1).

HG	
Phase	Wt. %
Gypsum	72
Dolomite	12
Calcite	5
Muscovite	3
Bassanite	3
Magnesite	2
Anhydrite	2
Quartz	1

Table 3: XRPD results of hydrated gypsum (HG).

HC	
Phase	Wt. %
C_3S+C_2S	13
C_4AF	6
Ettringite	4
Portlandite	14
Calcite	4
Am-unkn	59

Table 4: XRPD results of hydrated Contragress (HC).
Am-unkn =amorphous phases

HB	
Phase	Wt. %
C_3S+C_2S	7.0
C_3A cubic	< det. Limit
C_4AF	1.4
Ettringite	3.4
Portlandite	16.3
Hc (AFm)	1.0
Periclase	0.5
Calcite	2.2
Mc (AFm)	3.8
Am-unkn	64.4

Table 5 XRPD results of hydrated Blaue (HB)

In table 4, the hydrated Contragress (HC) contains unreacted C_3S and C_2S (13%). The existence of these phases means that the hydration of HC in one month was not complete. These phases can hydrate further. Ettringite was formed (4%) even though this cement is C_3A free cement. The ettringite was formed probably because of potential Al-impurities contained in the C_3S and C_2S (during the clinker production process).

In table 5, the hydration products of the hydrated Blaue (HB) are quantified. The ettringite was also formed (3.4%). Unreacted C_3S and C_2S exist as well and might further react and hydrate to produce C-S-H and portlandite (CH). AFm phases like hemicarbonate aluminates (Hc) and monocarbonate aluminate (Mc) were formed. These AFm phases form when the sulfate content in cement is consumed or reduced. They are unstable phases and might convert back into ettringite when further resource of sulfate is available again.

There was no ettringite formed in the hydration products of hydrated Fondu (HF), as expected because of lack of C_3S and C_2S as seen in table 6. From this table, it is also seen that the hydration mechanism and products are substantially different from those in Portland cement, other different phases as hydrogarnet and gibbsite are formed.

HF	
Phase	Wt. %
C$_4$AF	7.0
Hydrogarnet C$_3$AH$_6$	38
Gibbsite AH$_3$	17
CA	4
Magnesite Fe$_3$O$_4$	4
C2AS	2
Am-unkn	28

Table 6 XRPD results of hydrated Fondu (HF)

2.2 Methods

The investigation on the ISA phenomenon in this study is implemented using 4 different methods. The purpose of using these methods is to measure the early reactivity of the hydrated cement, the expansion in cement pastes or cement mortars and to quantify the crystallisation pressure after contamination with hydrated gypsum.

2.2.1 Length change measurements of mortar prisms

Fresh cement Fondu (F) was mixed with water and sand to cast mortar prisms. The sand (from the company Rohrdorfer) was sieved (<1 mm) and used to produce the mortar prisms. The water, sand and HG and fresh cements were weighted and mixed in the electronic mixer as previously explained (section 2.1.1). Table 7 shows the content of water, HG, sand and fresh fondu cement powder.
 The symbols in the table stand for: F= fresh fondu cement, 10 HG= 10% hydrated gypsum addition, f= fine hydrated gypsum particles and c= coarse cement particles, w/c ratio =0.65 or 0.50.
In a previous study [51], these effects were also investigated with different cement types. One of the cement types used was Der Blaue (B). These old prisms (only der Blaue because it showed high expansion) were also exposed to the new weathering cycles and the length change measurements are placed in the appendix.

Sample name	Water content (g)	Cement content (g)	Sand content (g)	Gypsum content (g)
F+0HG-0.5	225	450	1350	0
F+0HG-0.65	292.5	450	1350	0
F+5HG-c-0.5	225	450	1327.5	22.5
F+5HG-f-0.5	225	450	1327.5	22.5
F+5HG-c-0.65	292.5	450	1327.5	22.5
F+5 HG-f-0.65	292.5	450	1327.5	22.5
F+10HG-c-0.5	225	450	1305	45
F+10HG-f-0.5	225	450	1305	45
F+10HG-c-0.65	292.5	450	1305	45
F+10HG-f-0.65	292.5	450	1305	45

Table 7 Parameter investigated in the prism length change

For example in the mixture (F+0HG-0.5), 225 g of water, 450 g of fresh cement fondu, 1350 g of sand and 0 g of HG were used. The w/c was 0.5 (225 g of water and 450 g of cement) and there was no contamination with HG. This sample was considered as a reference sample. To investigate the effect of increasing w/c ratio to 0.65, the sample (F+0HG-0.65) was casted. The water content in this sample was increased to 292.5 g. In the mixture (F+5HG-c-0.5), the sample was contaminated internally with 22.5 g of fine HG. The additional amount of HG was subtracted from the content of the sand. All of the samples were let hydrate for 1 month in climate chamber, then they were exposed to drying wetting cycles.

The weathering cycles consisted of 2 days of heating in oven to 60 °C and 5 days wetting in ambient temperature water and lasted for 42 days long. The length change was recorded after the end of each cycle. For each investigated parameter, three replicates were casted. The length change was then the average of length change of these replicates. Figure 10 shows few of the casted prisms with 3 replicates for each investigated parameter.

Figure 10 Mortar prisms of fresh cement Fondu (F)

Each group of prisms (3 replicates) was submerged seperately in water container. In this way each group was stored separated avoiding the potential leaching of HG form other group into the submersion water [23].

The prisms in the oven (represent drying cycles) and in the water containers (represent the wetting cycles) are shown in the next figures (11-12).

Figure 11 Mortar prisms (F and B) in the oven exposed to the heating cycles (60°C)

Figure 12 Mortar prisms (F and B) in the oven exposed to the wetting cycles (60°C)

The expansion of the prisms is measured as following:

$$expansion = \frac{L_n - L_0}{L_0} \, x \, 100$$

L_0 is the reference length of the prisms before starting the weathering cycles and L_n is the length after each one of the 5 weathering cycles.

2.2.2 Rheological tests

We use rheological oscillatory tests to measure the elasticity regime and early reactivity of the hydrated cements with and without internal contamination with HG. The rheological tests were made using Anton Paar stress-controlled rheometer (MCR302).
The protocol used for the test consists of three steps:
- short time structuration (STS) for 60 seconds at a fixed strain (γ=0.001%) and frequency =1 Hz (preparation step)
- amplitude sweep (AS): γ=0.0005% to 0.005% and frequency= 1 Hz (less than 1 minute)
- Long-time structuration (LTS): 1 hour at γ=0.001% and frequency= 1 Hz

As already mentioned, AS was used for defining the linear viscoelastic regime and to impose small oscillation without destroying the structure of the dense suspensions in the LTS. Therefore, a range of amplitude strain oscillations was imposed, and storage (or elastic G') and loss (or viscous G'') moduli were measured.

LTS was conducted to follow the early hydration of the paste to verify if some chemical reaction is going on in the paste (i.e., secondary ettringite formation). For the small oscillations in LTS, the linear elastic modulus was obtained by averaging the G' plateau value and is linked to the cohesivity of the slurry. The critical strain was also obtained, and it responds to a drop in linear elastic modulus (80% drop in G'_{lin}). This critical strain is linked to the deformability of the paste [52].

The evolution of these moduli with the imposed strain is illustrated in figure 13 [1].
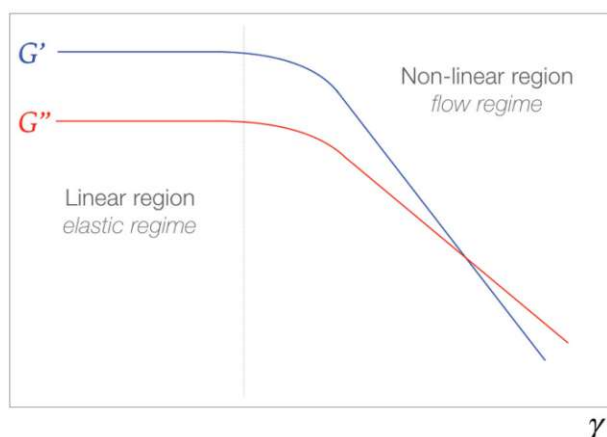

Figure 13 Evolution of G' and G'' as a function of the deformation in small amplitude sweep [1]

We tried to select the same initial cohesion (G') for all the investigated hydrated cements (before adding HG) and the rheological tests were made for these samples shown in table 8.

Cement type	Mixture name	Cement content (g)	Water content (g)	HG content (g)	Assumed $\emptyset$ $\emptyset = \dfrac{v_{hydrated\ solid}}{v_{total}}$
Hydrated Der Blaue (HB) (w/c=0.5)	HB+0HG	10.0	5.0	0.0	0.465
	HB+5HG	9.5	5.0	0.5	0.472
	HB+10HG	9.0	5.0	1.0	0.478
	HB+25HG	7.5	5.0	2.5	0.496
Hydrated Der Contragress (HC) (w/c=0.6)	HC+0HG	10.0	6.0	0.0	0.420
	HC+5HG	9.5	6.0	0.5	0.427
	HC+10HG	9.0	6.0	1.0	0.433
	HC+25HG	7.5	6.0	2.5	0.451
Hydrated Der Fondu (HF) (w/c=0.4)	HF+0HG	10.0	4.0	0.0	0.521
	HF+5HG	9.5	4.0	0.5	0.527
	HF+10HG	9.0	4.0	1.0	0.534
	HF+25HG	7.5	4.0	2.5	0.552
85% HB + 15% HF (w/c=0.6)	HB+HF+0HG	10.0	6.0	0.0	0.420
	HB+HF+5HG	9.5	6.0	0.5	0.427
	HB+HF+10HG	9.0	6.0	1.0	0.433
	HB+HF+25HG	7.5	6.0	2.5	0.451

Table 8 Mixtures of the cement slurries tested in the rheometer
w/c: water/cement ratio

It can be noticed from table 8 that the water content stays constant, but the content of added cement and HG vary. The solid volume/ total volume (Ø) varies as a result. The density for all the hydrated cements were assumed= 2.3 and for HG= 1.5 to calculate Ø.

The components of the cement slurry mixtures (hydrated cement, water, and HG) were weighted with Kern PCB weighted (0.01 g measuring accuracy). The cement and HG were dry mixed using small electronic mixer (Ultra Turrax TD300, IKA) for one minute to homogeneously blend the HG and cement particles. Distilled water was added carefully, and the blend was mixed again for 3 minutes (with 6000 rpm mixing speed). Figure 14 shows the mixer used for the rheological tests.

Figure 14 The mixer used for rheology tests

A blended cement was made by mixing 85 % of HB and 15% of HF by weight. This blended cement according to the literature is expected to form considerable amount of ettringite and causes expansion either with or without addition of HG [16]. For each cement sample, the test was repeated two times for the purpose of reproducibility.

A plate-plate geometry PP25 P2 and moisture chamber (to reduce water evaporation) were used. The temperature of the rheometer was kept at 22°C. Figure 15 shows the used geometry during the rheological test of one cement slurry.

Figure 15 sample of cement slurry during the rheological tests

2.2.3 Le Chatelier expansion rings

This method was modified in this study to investigate the expansion of hydrated cement pastes by addition of (hydrated) gypsum. The same mixtures used for the rheology tests (see table 8) were used here for producing the cement pastes to examine the expansion in LC rings. The contents were weighed to produce more cement pastes to fill the LC rings (30 mm h x 30

mm diameter) and the weight percentage of each component of the mixture stayed ident to the one used in table 8.

The mixing procedure was also identical to the one in rheology tests, except a bigger electronic mixer was used (model IKA starvisc 200-2.5 with maximum speed of 800 rpm). Figure 16 shows the mixer used to prapare the cement pastes for LC tests.

Figure 16 Mixer used for preparing LC samples

After the mixing was completed, the cement paste was casted in the rings and let set for one day. The rings were covered with plastic sheets to prevent the water evaporation. After that the ring was placed inside a frame from plexiglas with about 1.5 mm tolerance. This setup was placed in water at ambient temperature for one month and the distance between the needle was recorded in time intervals for about 1 month (after 1,4,7,11,17,21,25-day). Each LC ring was submerged in a separate water container to avoid leaching of ions from different cements in the submersion water. In this way contamination with other materials was prevented [23]. With the confined geometry, the vertical expansion was prevented. For significant expansions the test was repeated twice for the purpuse of reproducibility. The LC rings with the investigated cement pastes are shown in figure 17.

Figure 17 LC rings with cement paste samples

The distance between the needles of LC rings directly after one day of placement of the cement paste in the ring is L_0. As the cement paste in LC rings expands (or shrinks), the distance between the needles will increase and the distance is called L_n. The relative deformation of the cement paste is then expressed by the following relationship:

$$\text{rel. deformation} = \frac{L_n - L_0}{L_o} * 100\%$$

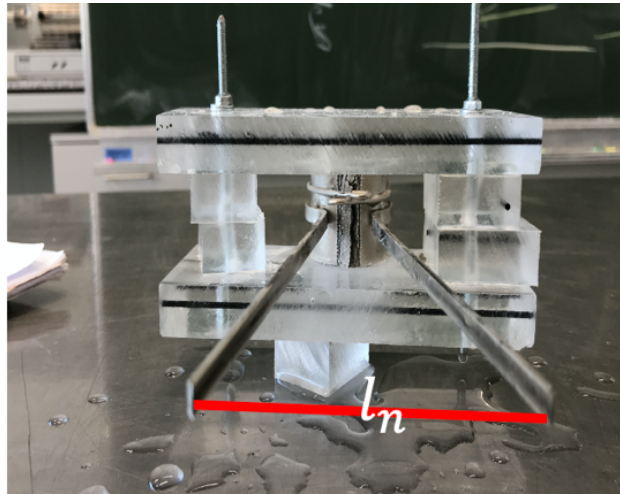The distance between the needles after the expansion (L_n) is shown in figure 18.

Figure 18 LC expansion: distance between the needles after expansion

2.2.4 Oedometer

As already mentioned, the idea of using this device was to measure the crystallisation pressure resulted from (secondary) ettringite formation (leading to swelling). The confinement of cement paste in axial direction allows the cement to expand only vertically. The stress resulted from this expansion can be registered, and the damage extent can be anticipated by comparing the tensile strength of the cement with the registered stress.

A setup of thermal water bath was integrated into this device to expose the cement paste to weathering cycles of heating to 60 °C and then lowering the temperature to 20 °C. This way, the physical sulfate attack could be simulated. The deterioration could be accelerated because the ettringite is dissolved in the heating cycle and recrystallise upon cooling. The thermal bath setup is shown in figure 19.
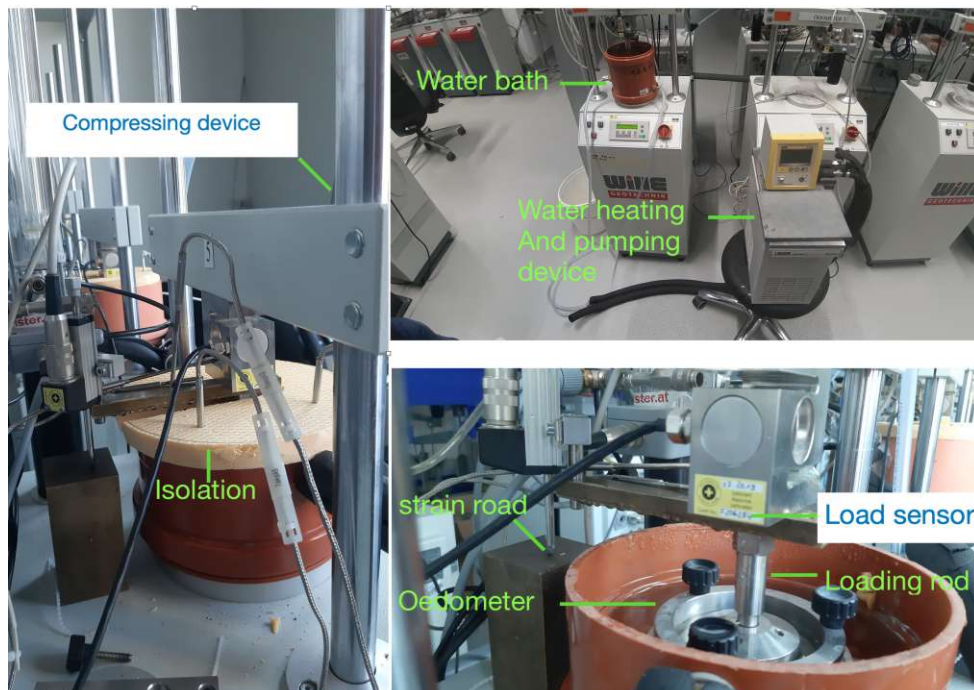

Figure 19 Oedometer device with the integrated water bath
Courtesy to Mr. Andreas Hausenberger

On the right upper photo in figure 19, the sample with the oedometer was placed inside the water bath. The water temperature was regulated by the heating/ pumping device (Huber Ministat 125) and the water was pumped into the water bath. On the right lower photo, the position was hold constant by placing the strain road outside of the setup to avoid heating it with the water and consequently to avoid false measurement (it was one of many trials to understand the temperature effect on the results). The loading rod was in contact with the sample inside the oedometer and it was also affected by the water temperature increase.

On the left side photo, a simple isolation was integrated and placed above the water bath to prevent the water vapour condensation into the load sensor and to avoid heating of the loading sensor (both cause error measurements). To test the response of the oedometer to the temperature change, different material were used in this study. Plexiglas is a material which is sensitive to temperature and expands upon temperature raise. The other used materials were thermal stone and steel, which are relatively highly resistant to temperature change, and are expected not to suffer voluminous change upon heating to 60°C.

The oedometer showed very high sensibility to temperature change in all of the investigated samples.The expansion phenomenon in ISA is also sensitive to changes in temperature. Due to the double temperature effect, the crystallisation pressure obtained by the oedometer will be therefore inaccurate.The problems affecting the reliabiity of the results could be summerised as the following:

- Water turbulance: the water was pumped into the sample and the load sensor could detect the movement of the water inside the water bath, which in return affects the results.
- The temperature of the water: the water vapour condensation on the loading cell, the heating of the strain and loading rods and the loading cell affected the results significantly. This requires loading rod of special material insensitive to temperature variation and special isolation system to prevent condensation.

The failing test to calibrate the oedometer made the testing of hydrated cement samples impossible. The results of the calibration tests are shown in appendix.

3. Results and discussion

3.1 Length change measurement of the mortar prisms

The results of length change measurements are shown in the next figures (20-22). The x-axis shows the measurement time, while the y-axis shows the expansion. The expansion is calculated as the average of the 3 replicates, with the resulting error bar. In the beginning (day 0), the expansion is 0% and the initial length of the prism is the reference length.

In the figure 20, the expansion of the Fondu mortar prism without HG addition and with w/c=0.5 and w/c=0.65 is shown.
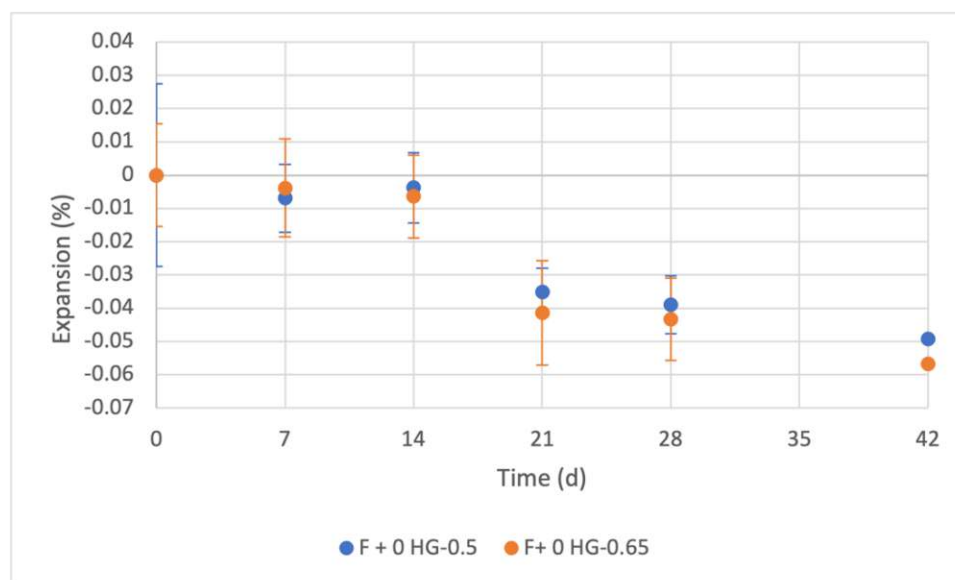
Figure 20 Expansion of the mortar prisms
F + 0 HG-0.5: Fondu+ 0 hydrated gypsum and w/c=0.5, F+ 0 HG-0.65: Fondu + 0 hydrated gypsum and w/c=0.65

All the prisms start to shrink in the first cycle (day 7). The prisms with w/c=0.65 show higher shrinkage relative to the ones with w/c=0.5.
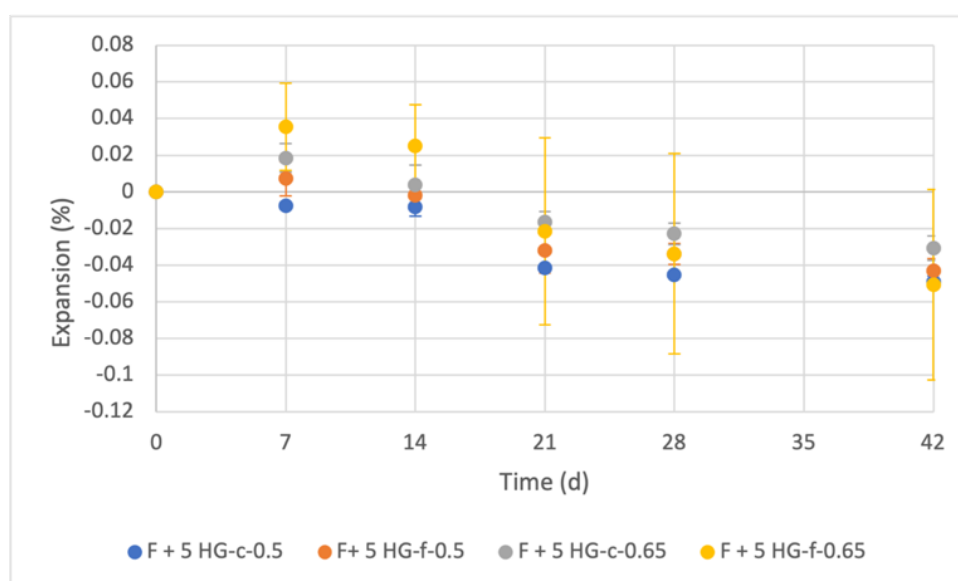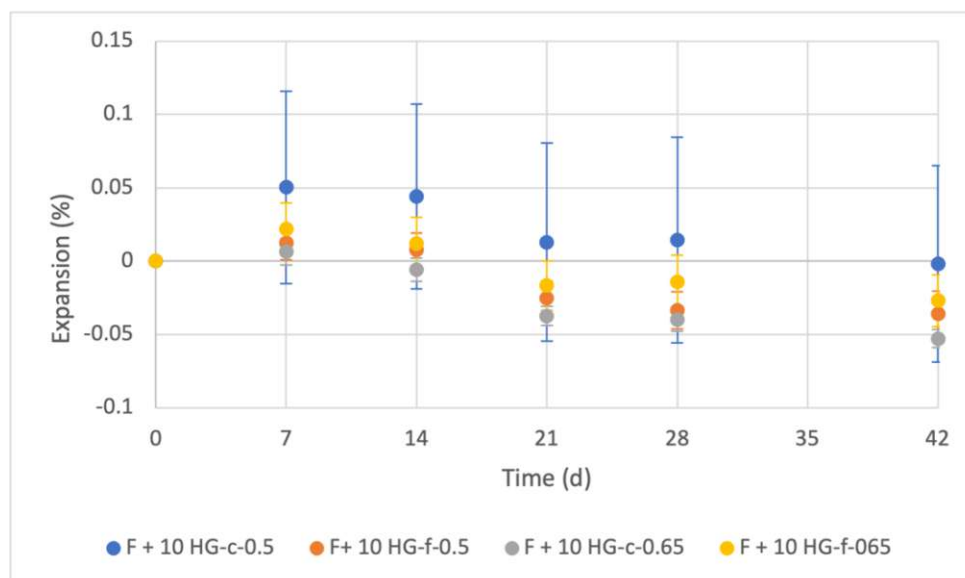

Figure 21 Expansion of the mortar prisms
F + 5 HG-c-0.5: Fondu+ 5 hydrated gypsum, c= coarse gypsum and w/c=0.5,
F+ 5 HG-f-0.5: Fondu + 5 hydrated gypsum, fine gypsum and w/c=0.5,
F+ 5 HG-c-0.65: Fondu + 5 hydrated gypsum, coarse gypsum and w/c=0.65,
F+ 5 HG-f-0.65: Fondu + 5 hydrated gypsum, fine gypsum and w/c=0.65

In figure 21, the expansion of the prisms with 5 HG addition, fine and coarse HG and two w/c ratios (0.5 and 0.65) is shown.

The sample F + 5 HG-c-0.5 start to shrink continuously from the first cycle (day 7) until the end of the test. The other samples expand in the first cycle and the value of the expansion for each of them is reduced continuously after each cycle. All the samples show shrinkage starting on the 3rd cycle (day 21).

In figure 22, the expansion of the prisms with 10 HG addition, fine and coarse HG and two w/c ratios (0.5 and 0.65) is shown.

Figure 22 Expansion of the mortar prisms
F + 10 HG-c-0.5: Fondu+ 10 hydrated gypsum, c= coarse gypsum and w/c=0.5,
F+ 10 HG-f-0.5: Fondu + 10 hydrated gypsum, fine gypsum and w/c=0.5,
F+ 10 HG-c-0.65: Fondu + 10 hydrated gypsum, coarse gypsum and w/c=0.65,
F+ 10 HG-f-0.65: Fondu + 10 hydrated gypsum, fine gypsum and w/c=0.65

All the samples show expansion in the 1st cycle and the value of the expansion is reduced continuously after each cycle until the end of the test. The sample F + 10 HG-c-0.5 shows the highest value on expansion.

The only clear trend noticed is that the prisms without HG and with w/c= 0.65 shrink more than the ones with w/c=0.5. The higher w/c ratio means that more amount of water will be available than necessary for the cement to complete the hydration. Some water will be bound in the structure of cement hydrates. The rest of water will increase the porosity inside the cement. Once the prisms are heated, the rest water will evaporate, and the prism will shrink.
 It is especially expected that HF show this shrinkage behavior when the used w/c is > 0.4 [16]. The conversion of aluminate phases will lead to producing of hydration products with less volume. The gibbsite converts to the more stable phase C_3AH_6 (less volume and higher density), water will be released to the matrix and the porosity increases [16, 53].
There is no general trend obtained for the effect regarding the amount of the HG addition or HG fineness. Small initial values of expansion of the prisms are noticed only by adding HG. The expansion is reduced after each weathering cycle, which was not expected. The testing time of 42 days is evidently too short for the prisms to show any significant expansion due to the ISA. As previously mentioned in the introduction, the SA causes expansion only after several years. The expansion values of der Blaue mortar prisms are shown in Appendix.

3.2 Results of rheological tests

The linear viscoelastic regime was measured for all the samples listed in table 8 and the elasticity and deformability of the samples measured through G'$_{lin}$ and γ_{cr} are shown in the next figures for the hydrated cements.

In figure 23 the the evolution of G'$_{lin}$ of the hydrated Contragress (HC) is plotted. The hydrated gypsum concentration (by weight) is plotted on the x-axis.
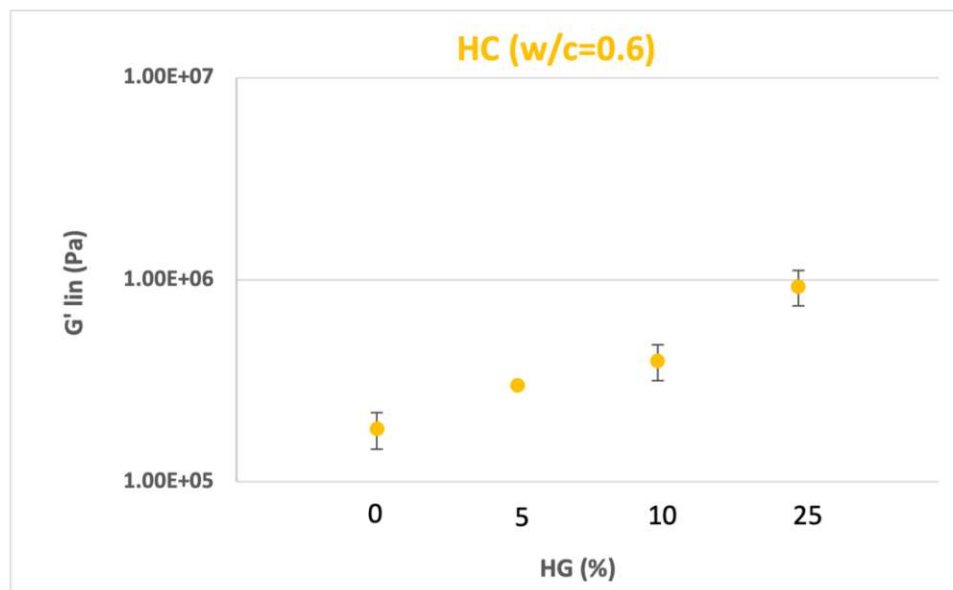

Figure 23 G'$_{lin}$ evolution for the hydrated Contragress (HC)

The (small) error bar shown in this figure represent the standard deviation for both of the replicates for the different HG concentration (5% only one sample). The G'$_{lin}$ increase gradulally by adding HG and reaches the maximaum value with 25% HG addition. This increase is probably due to the increased solid content (∅). The value of ∅ for 0, 5, 10 and 25% HG is 0.420, 0.427, 0.433 and 0.451, respectively.

Figure 24 shows the evolution of the G'$_{lin}$ for the hydrated Blaue (HB). Two samples were also tested to get reproducible results. The error bar for the sample with 5 and 10% HG is very small and cannot be seen in the figure.
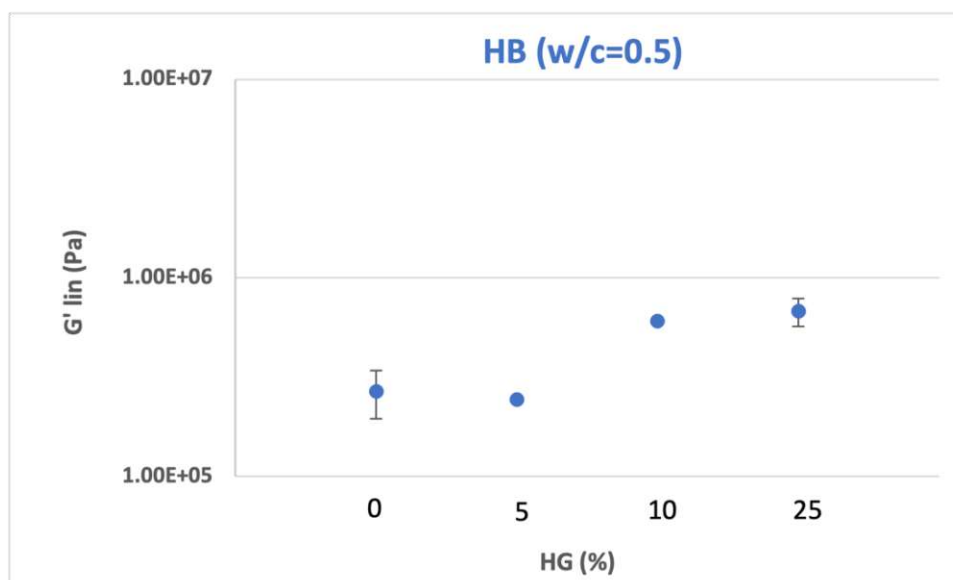
Figure 24 G' $_{lin}$ evolution for the hydrated Blaue (HB)

For this cement the 5% HG addition does not affect the value of G'$_{lin}$. The addition of 10% and 25% HG addition increase the value of G'$_{lin}$ to the same value probably due to the increased

solid content (Ø). The value of Ø for 0, 5, 10 and 25% HG is 0.465, 0.472, 0.478 and 0.496, respectively.

The increase of G'$_{lin}$ with respect to the HG concentration for hydrated Fondu (HF) is plotted in figure 25. Also here the error bar calculated for two samples. The value of Ø for 0, 5, 10 and 25% HG is 0.521, 0.527, 0.534 and 0.552, respectively.
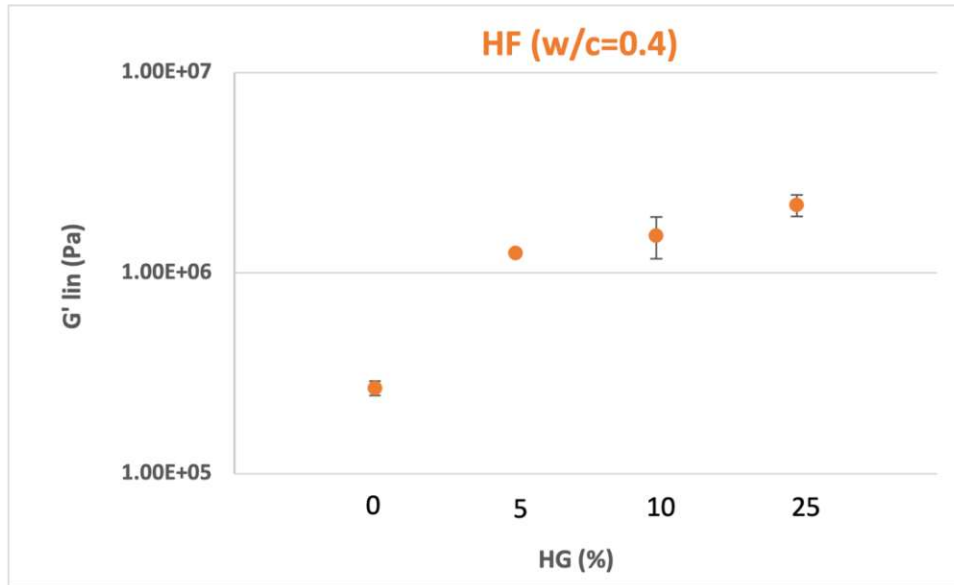

Figure 25 G' $_{lin}$ evolution for the hydrated Fondu (HF)

Figure 25 shows that HF is very sensitive to the addition of HG. Even with 5% HG addition, the G'$_{lin}$ increases significantly.

The G'$_{lin}$ evolution for the blended cement (85% hydrated Blaue+ 15% HF) with respect to the HG addition is shown in figure 26. The value of Ø for 0, 5, 10 and 25% HG is 0.420, 0.427, 0.433 and 0.451, respectively.

Figure 26 G'$_{lin}$ evolution for the hydrated Blaue (HB) 85% + hydrated Fondu (HF) 15%

This system shows an increase in G'$_{lin}$ only after 25% HG addition. For the other HG additions, no clear difference to the reference sample (0% HG) is noticed.

Figure 27 shows all of the hydrated cement together and how the HG addition influencethe cohesivity. It allows a quick comparison between all of the hydrated cements.
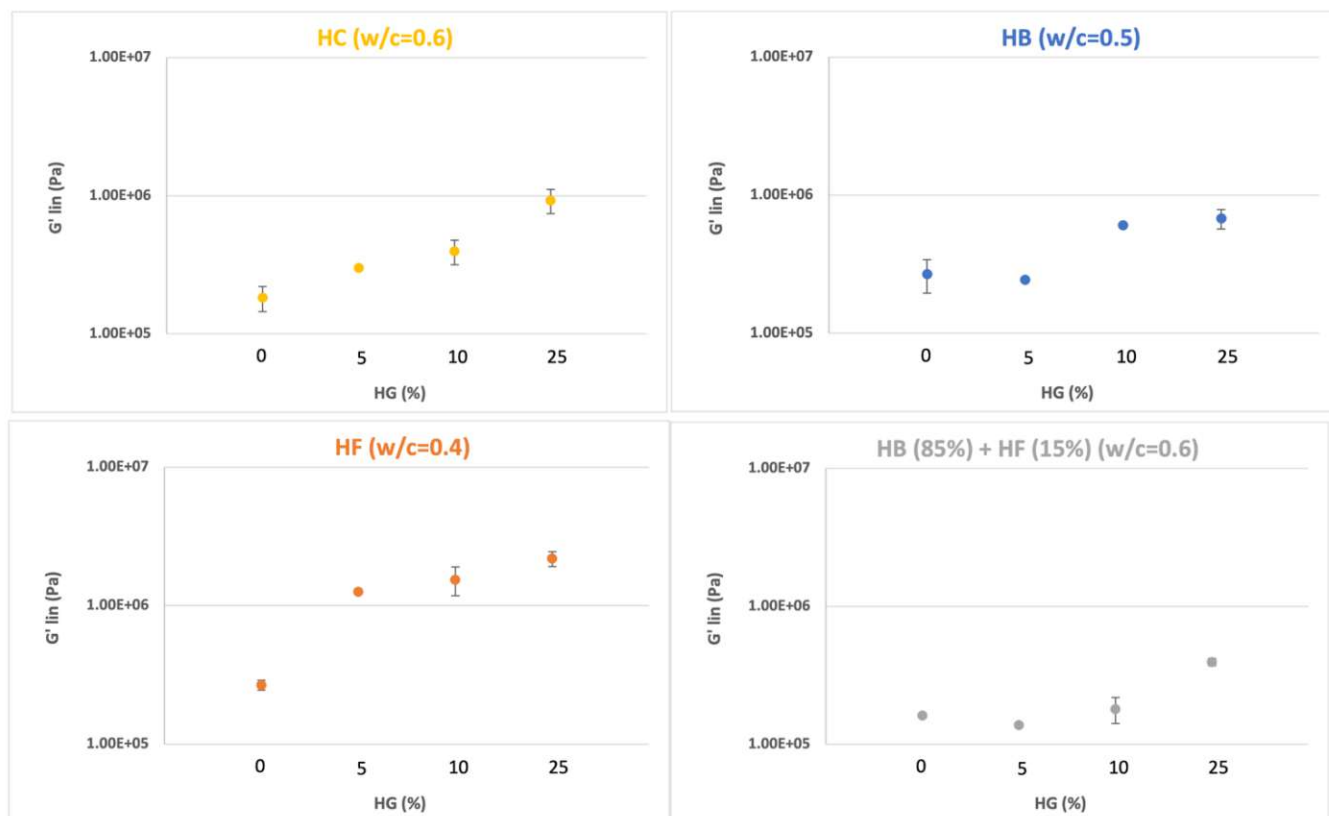
Figure 27 G'lin evolution for all the hydrated cements plotted together

The increase in G'$_{lin}$ can be attributed to the presence of additional powder. Comparing the behavior of the 4 pastes with different HG content tell us that for HF somenthing else can probably happen. The increase in G'$_{lin}$ is in fact suggesting a stronger early reactivity of the paste HF once HG is added. G'$_{lin}$ increases by about one order of magnitude when 25% HG is added.

The change in γ_{cr} with respect to HG concentration for HC is plotted in figure 28. The x-axis shows the HG concentration (**by weight**) and y-axis shows the evolution of γ_{cr} (**by percentage**).
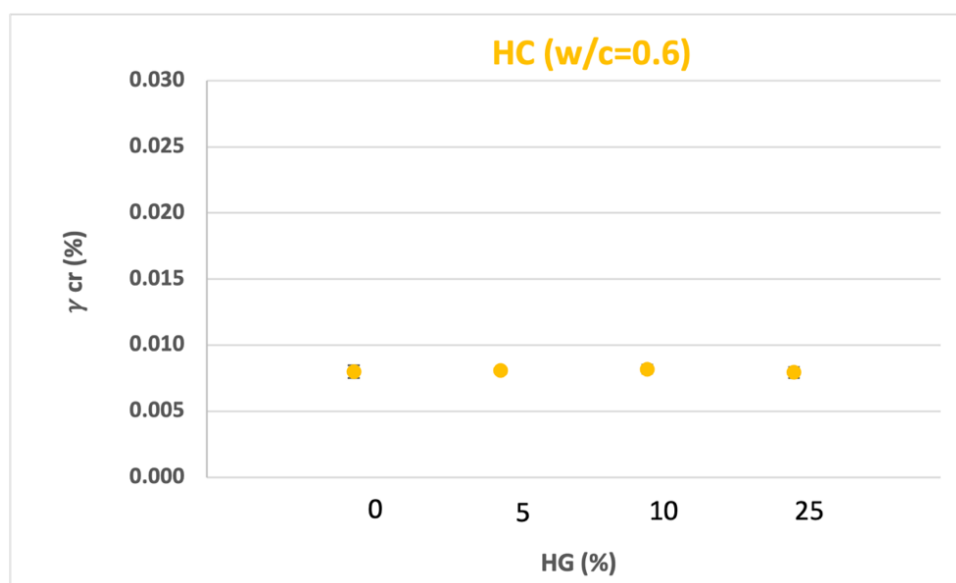

Figure 28 γ_{cr} evolution for the hydrated Contragress (HC)

No change is noticed in this figure for all of the concentrations of HG. The system maintain the same deformability. For HB, the evolution of γ_{cr} is shown in figure 29.
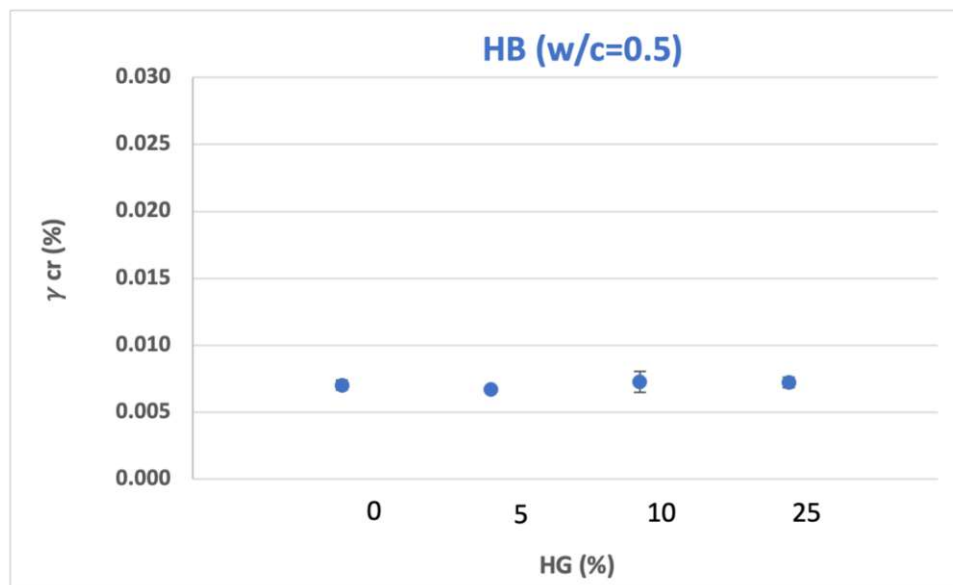

Figure 29 γ_{cr} evolution for the hydrated Blaue (HB)

The evolution of γ_{cr} for the system HB is similar to the HC. For all HG concentrations, no change is noticed.

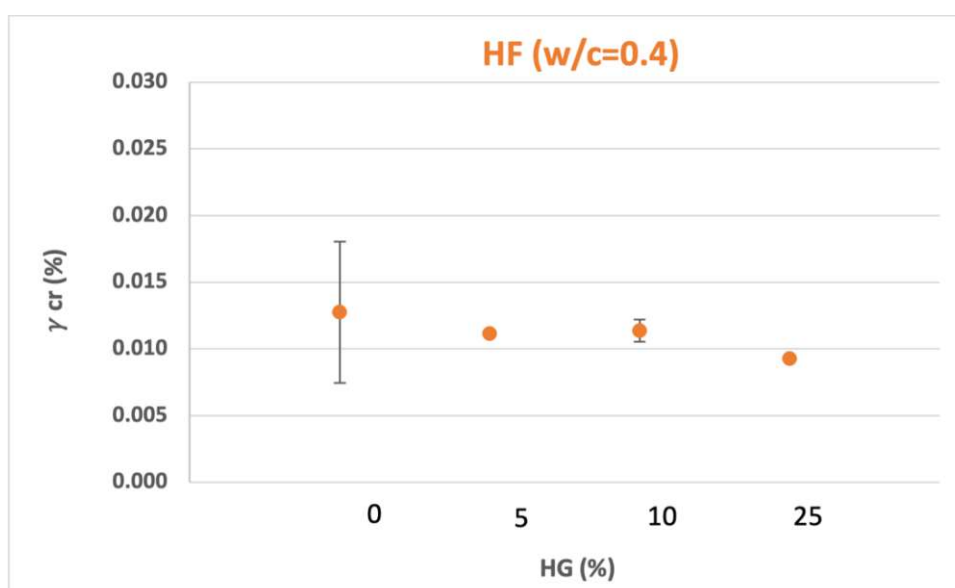For the hydrated Fondu, the evolution of γ_{cr} is shown in figure 30.

Figure 30 γ_{cr} evolution for the hydrated Fondu (HF)

It can be seen from figure 30 that the γ_{cr} slightly decreases with increasing the HG%. The system develops a negligible fragility by adding HG.

For the blend (85% HB + 15% HF), the change in γ_{cr} is shown in figure 31.

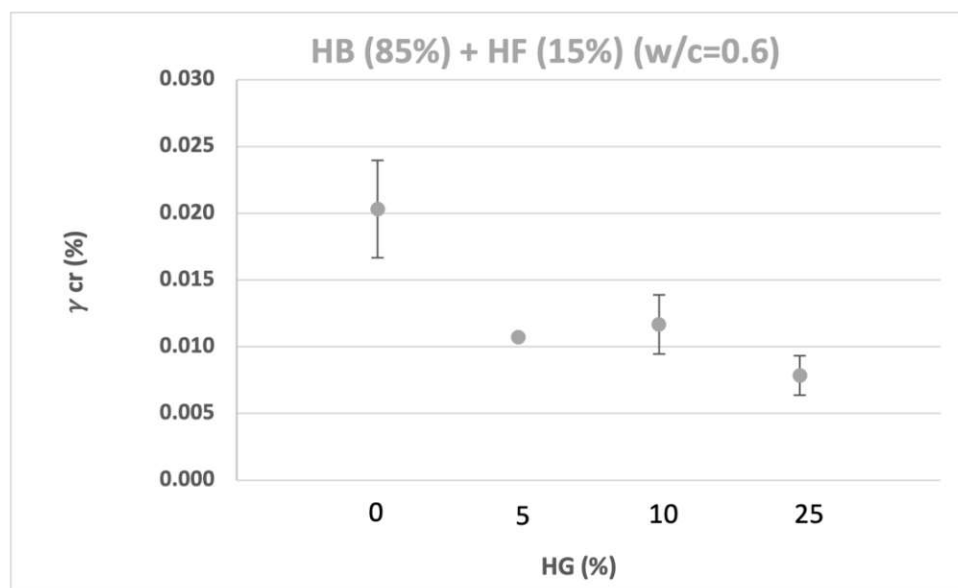*Figure 31 γ_{cr} evolution for the hydrated Blaue (HB) 85% + hydrated Fondu (HF) 15%*

The system HB+HF shows the highest decrease upon addition of HG. This means that this system is getting more fragile by increasing the HG concentration.

For the purpose of a quick overview and comparisons between the systems, figure 32 shows the change in γ_{cr} for all of the hydrated cements together.
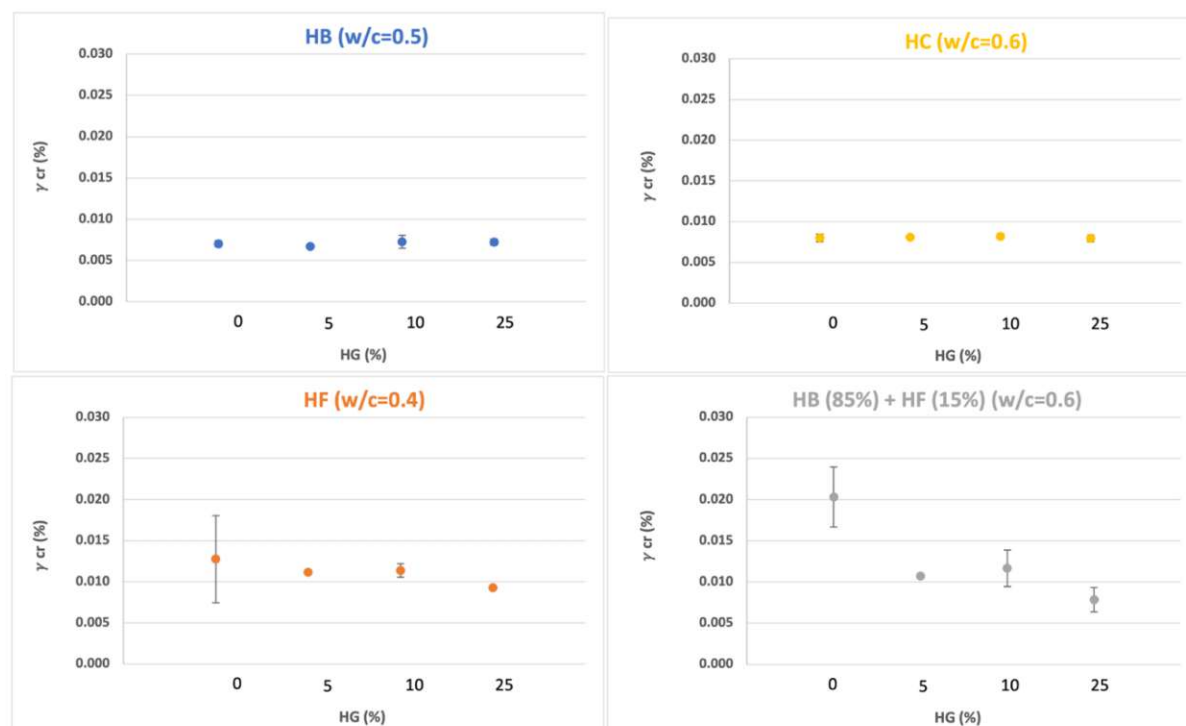

Figure 32 γ_{cr} evolution for the hydrated cements together

The evolution of γ_{cr} for HB, HC and HF is insignificant and therefore these hydrated cements show the same deformability with 0, 5, 10 and 25% HG. The hydrated cement (HB+HF) shows the highest decrease in γ_{cr} by adding HG and the structure is fragilized. One reason for this fragility is probably that C_3S dissolution and precipitation is delayed or prevented by the addition of HF and HG. The system can show a lower early strength evolution being more sensitive to any voluminous change (i.e., formation of ettringite) [16, 22, 54].

Now, the result from the long-time structuration which show the evolution of the cohesion with time (i.e., early reactivity) of the pastes are shown in the next figures (33-38).

Figure 33 shows the long time structuration (LTS) so the evolution of storage modulus (G') with time for HC and with different HG concentrations. The time in seconds is shown on the x-axis and the the storage modulus (G') is shown on the y-axis. Two tests are repeated for the HG concentrations (0, 10, 25%) and the results for both tests are very similar (high reproducibility). The error bar is shown only in the initial point to enable clear plotting of the figures.
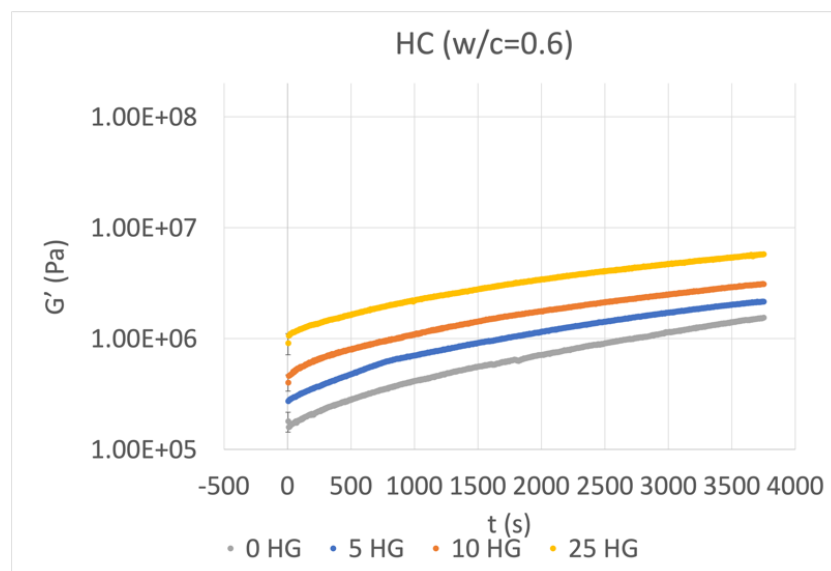

Figure 33 LTS for hydrated Contragress (HC) for 0, 5, 10 and 25% HG addition

It can be seen from figure 33 that for 0 HG, the G' of HC increase with time. As already mentioned, the reason for this reactivity can be that the unreacted C_3S and C_2S (see table 4) rehydrate with water and preciptate further hydration products. By adding (5, 10 and 25%) HG by weight, the initial G' value probably increases due to an increase in the solid content (increase in $\emptyset$, see table 8), as also observed in the G'$_{lin}$. The slope of G' is more or less the same both by adding 25% HG and by 0% HG. This suggest that adding HG did not increase the reactivity of HC. It is expected in HC that no (secondary) ettringite forms upon addition of HG because HC is C_3A free cement.

The evolution of G' for the HB is shown in figure 34. The error bar is very small due to high reproducibility of the results for this system.

By 0% HG addition, the HB shows some higher reactivity than HC. The exitence of remainang unhydrated C_3S and C_2S and also the AFm phases is probably the reason for this reactivity (see table 5). Further precipitationf of hydration products might result from the dissolution of C_3S and C_2S. It is not known whether the AFm phases will transform to ettringite by addition of HG%. For this an XRD analysis need to be performed. Nevertheless, it is expected according to the literature that the transformation of AFm phases to ettringite will occur upon addition of HG [19]. The addition of 5% HG decrease the reactivity of HB, and further decrease is caused by adding 10% HG. These decrease in reactivity in the first hour by adding HG can be interpreted with a slow down of further hydration of residual C_3S and C_2S. The initial increase in G' is probably caused due to the increase in $\emptyset$ as already mentioned for G'_{lin} .
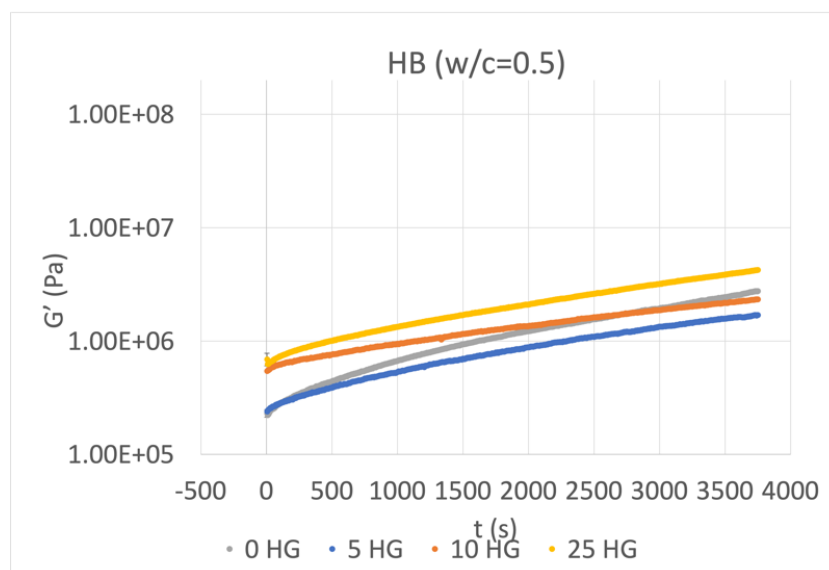
Figure 34 LTS for hydrated Blaue (HB) for 0, 5, 10 and 25% HG addition

The evolution of G' with time for the HF is shown in figure 35.
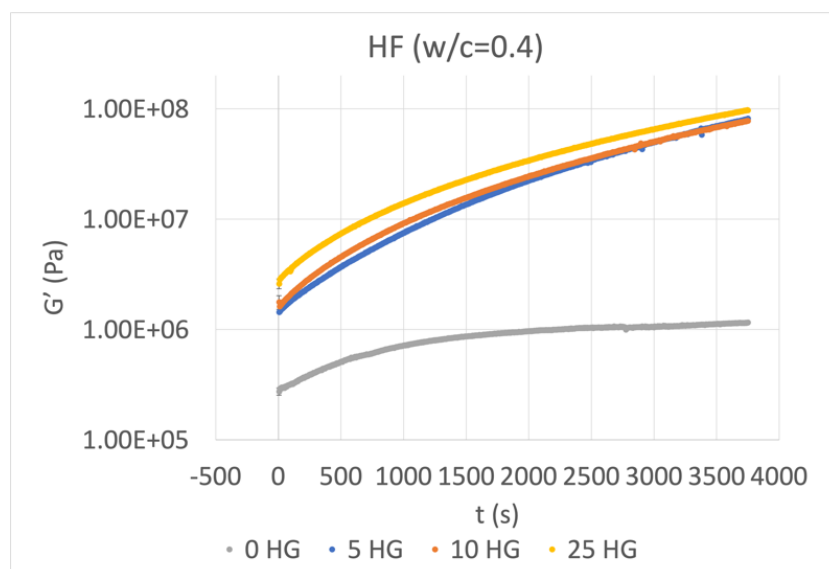The cement HF shows a significant reactivity upon addition of HG. The increase in the HG

Figure 35 LTS for hydrated Fondu (HF) for 0, 5, 10 and 25% HG addition

concentration (from 5, to 25%) does not significantly affect the evolution of G' in the first hour of testing.

The higher amount of available aluminate (without any C_3S and C_2S) assure the fast precipitation of new hydration product (secondary ettringite is mostl likely precipitate according to the literature) in presence of HG, resulting in a high increase in G'. In accordance with the literature [16] we also expect this cement to harden and set faster than HB and HC.

The evolution of G' with time for the blend hydrated Blaue and hydrated Fondu (85%HB+15%HF) is shown in figure 36.

The blend HB+HF reacts the highest by 0% HG addition as observed in the HB system. Here, the presence of HF makes the difference between the reactivity of the system without gypsum and that with gypsum more evident. This encourage our hypothesis that in presence of an excess of sulfate, C_3S and C_2S hydration is delayed. At the same time the presence of aluminate fragilize the system by the formation of secondary ettringite. In order to verify these hypotesis, an in situ XRPD (on cement paste) analysis is needed together with calorimetry tests to measure how the heat of the reaction develops. By comparing the heat resulted from

this reaction with the one results from pure ettringite or AFm formation (value of enthalpy from the literature), a further understanding can be reached.
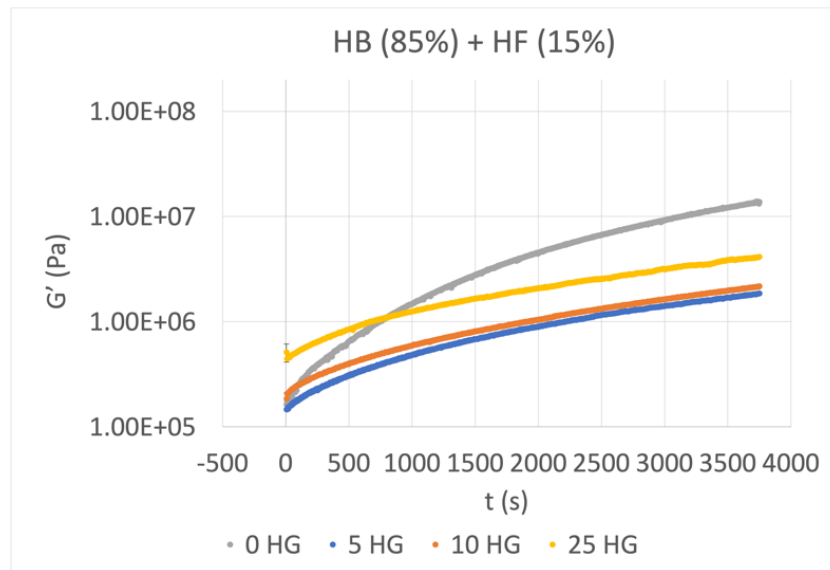

Figure 36 LTS for hydrated Blaue + hydrated Fondu (HB + HF)
for 0, 5, 10 and 25% HG addition

The evolution of G' with time in LTS for the 4 investigated hydrated cements is plotted in the figure 37 for the purpose of quick overview and comparison.
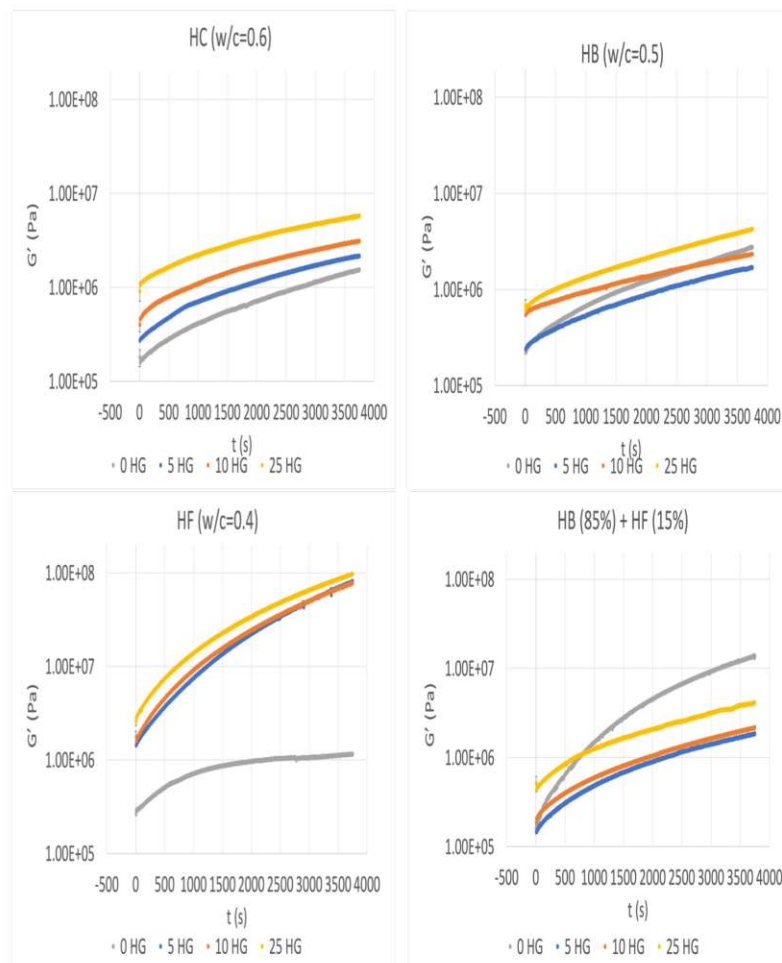

Figure 37 LTS for all the hydrated cements
for 0, 5, 10 and 25% HG addition

The initial increase in G' in all the systems can be attributed to both an initial fast reaction of the unhydrated phases and/or the increase of the solid content by HG addition. The HF shows the highest reactivity when HG is added. Decreased reactivity in both HB and HB+HF is noticed.

In the course of obtaining these results, a question was raised: is the increase in G' caused by the reactivity of the hydrated cement with the gypsum (chemical reactions) or is it due to the hardening of the gypsum itself? To answer this question, an additional test was made. The evolution of G' for pure HG upon mixing with water (water/gypsum ratio: w/gypsum= 0.67) was measured for one hour. The result was then compared with the G' evolution of pure HF and with HF+25% HG (water/cement ratio w/c= 0.4 for both) as shown in figure 38.
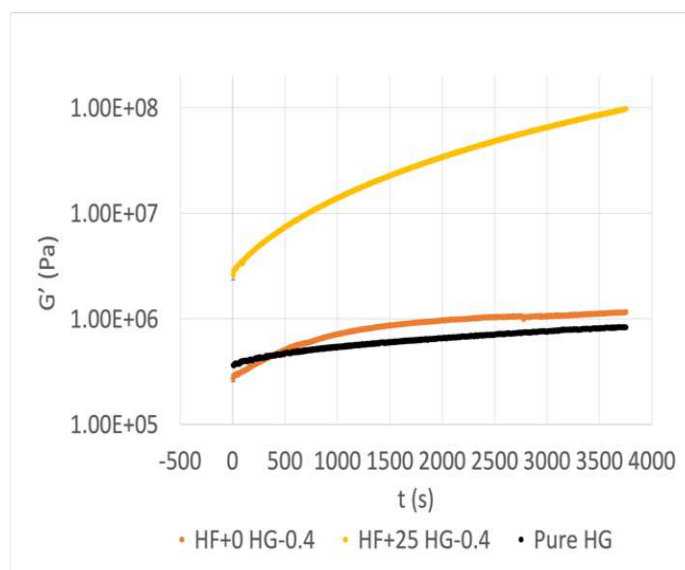

Figure 38 LTS for pure HF (0% HG, w/c=0.4)
vs. HF+ 25% HG (w/c=0.4) vs. pure HG (w/gypsum= 0.67)

 The comparison between these three systems show that pure HG is not highly reactive with water (no significant raise in G'). The HG has fully hydrated and by remixing with water no major additional hydration occurs. A chemical reaction between the HG and HF is definitely the cause for the raise in G'. Precipitation of hydration products like secondary ettringite are likely to occur. The ettringite binds up to 85% of water in it's structure [16]. This means that most of the hydration water will be consumed to hydrate ettringite. As a rsult, fast drying of the cement paste, fast setting and a raise in G' will occur.

3.3 Results of LC expansion rings

As previously mentioned in section material and methods, the mixtures used in the rheological tests (table 8) were prepared again to test the expansion in LC rings for longer times (i.e., days). The relative deformation of the LC needles for all the hydrated cements and for 0 HG% addition is plotted in figure 39. The x-axis shows the time of the reading with the caliper (in days) and the y-axis shows the relative deformation (%). All the measurement started after one day of the placement of the pastes in LC rings.
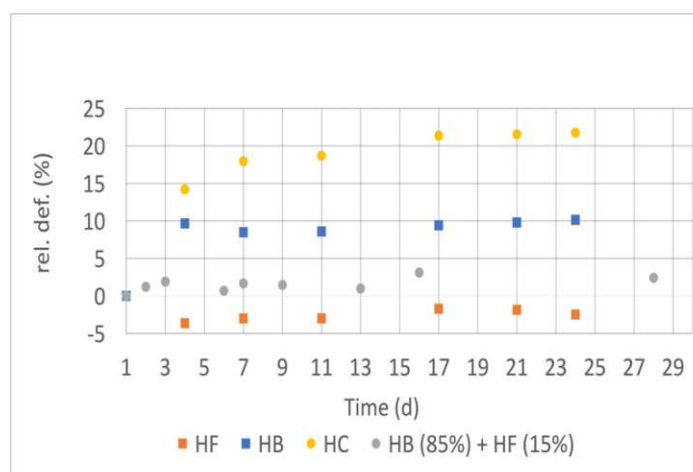
Figure 39 expansion of hydrated cements in LC with 0% HG
w/c= 0.4 for HF (hydrated fondu), 0.5 for HB (hydrated Blaue), 0.6 for HC (hydrated Contragress) and 0.6 for
HB+HF (85% hydrated Blaue + 85% hydrated Fondu)

The HC shows a relative deformation of about 20% at the end of the test (this expansion is not expected and it is probably related to a problem in the setup. In a previous study [51], the prisms of fresh Contragress did not show any expansion). The HB shows only a minor expansion (10%) after a few days from the placement and stay constant in volume for the rest of the testing time. The blend HB+HF shows about 2% expansion and the value stays constant for the whole testing time. The HF shows instead a minor shrinkage of about 3% at the end of the test as already observed in F prisms.

The expansion for all the cements with 25% HG addition is shown in figure 40.

This figure is zoomed in twice to clearly show the amount of expansion for HF, HC (zoom 1) and for HB (zoom 2).

For both HC and HF, no or only negligible expansion is noticed at the end of the test. The expansion is 3% for HF and 2% for HC in the last day. The sample (HC) shrink in the first 12 days. On the other hand, the paste HB continues to expand during the whole time of testing. The value of the expansion reaches 19% in the 4th day and 60% in the last day of the test. The blend (HB+HF) shows the highest expansion with the value of the expansion reaches 169% in the 4th day and 985% in the last day of the test. The increased fragility (decrease in γ_{cr}) of this system as already shown in rheological result section explains the high values of expansion in this hydrated blended cement.

The cement HC is free from C_3A and is considered as resistant to sulfate attack. It shows therefore only negligible expansion in presence of HG. HC shrinkage (in the first 12 days) is probably due to the lack of confinement as shown in figure 41.
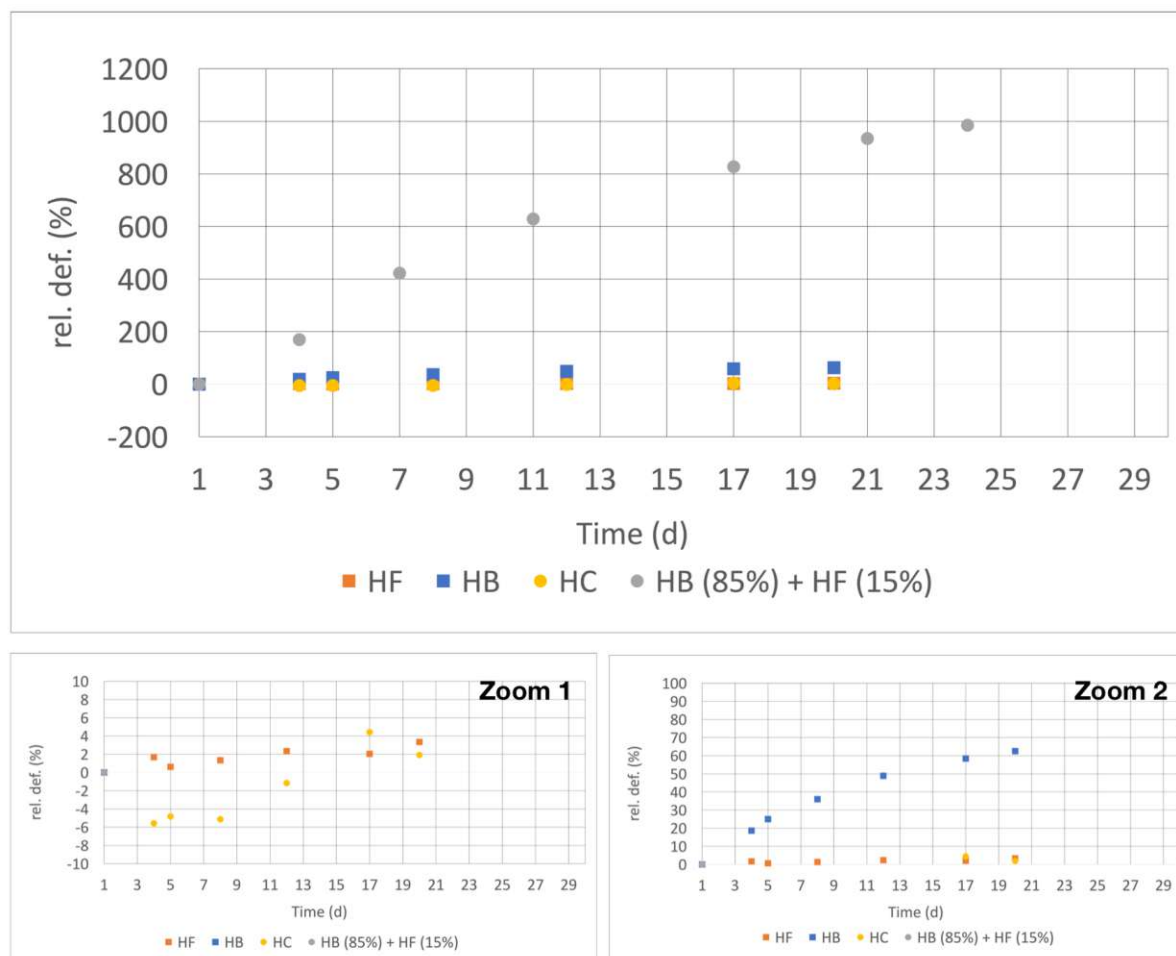
Figure 40 expansion of hydrated cements in LC with 25% HG
w/c= 0.4 for HF (hydrated fondu),
0.5 for HB (hydrated Blaue),
0.6 for HC (hydrated Contragress) and
0.6 for HB+HF (85% hydrated Blaue + 85% hydrated Fondu)

Figure 41 Lack of confinement in hydrated
Contragress (HC + HG)

This cement does not expand significantly, there is a gap of about 1.5 mm between the top
Plexiglas and the top of the ring. The sample is also not levelled well with the top of the ring.

In this way, the cement can move vertically and the distance between the needles will decrease, which will be measured then as if the sample shrinks.

Figure 42 shows the low consistency of HF without HG addition

Figure 42 low consistency of hydrated Fondu (HF)

HF shows high fluidity that makes the LC tests really difficult due to leakage of the paste. Even if the sample is placed carefully in the LC ring, the existence of the split allows the fluid paste to leak out. In this way the cement will not be levelled with the top of the ring after hardening. This means that for cements with low consistency and low expansion, no reliable measurement is obtained. Additionally for these paste if any expansion happens, it will be in the first day directly after mixing. In this period, the pastes are casted in the LC rings and let set for one day. Only after this, the LC rings can be placed in the frame without compromising leaking of the paste through the split.

Figure 43 shows the degradation of HF after 52 days of hydration.

Figure 43 Degradation of hydrated Fondu (HF)

It can be seen from this figure that HF degrades even after long time of hydration. At the end of the test, the cement can be easily scratched by finger.

The cement HB is ordinary Portland cement and considered having a low resistance to sulfate attack. The addition of HG is supposed to form ettringite, and the ettringite formation is accompanied by volume expansion [26, 54]. The expansion here is probably due to the

transformation of the AFm phases existed in the HB into secondary ettringite after addition of HG .

As already shown, the blend HB + HF + 25 HG shows the highest expansion. Figure 44 shows both of HF and the blend (HB+HF) in the end of the testing time. Both are contaminated with 25% HG.
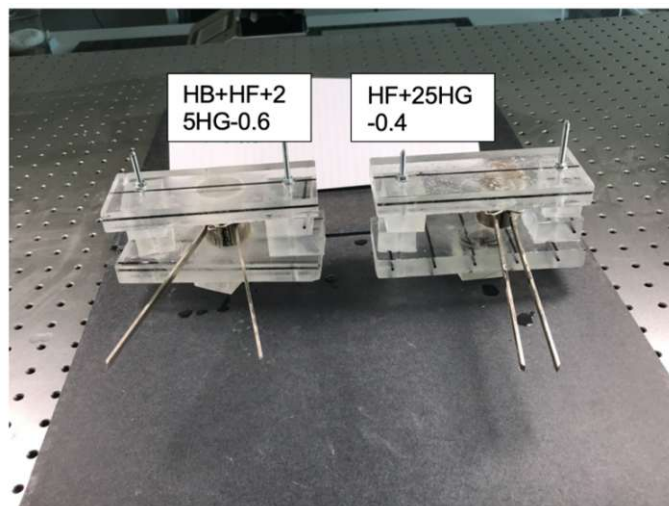

Figure 44 The expansion of HF vs. HF+HB
HB + HF +25 HG-0.6:
(85% hydrated Blaue+ 15% hydrated Fondu) + 25% hydrated gypsum and w/c=0.6,
HF + 25 HG-0.4: hydrated Fondu + 25% hydrated gypsum and w/c=0.4

The big distance between the LC ring indicators explains the significant expansion values of the system HB+HF+HG shown here. This system according to the literature [16, 55] is supposed to form significant amount of ettringite. It is also expected to damage in this way if the HG or HF/HG ratio is not carefully chosen. The expansion of this blend with 25% HG addition was repeated twice and the results are shown in figure 45.
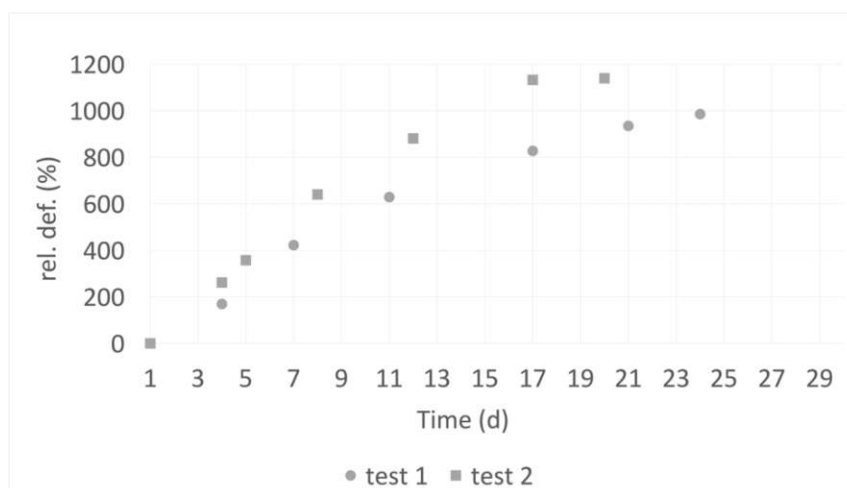

Figure 45 expansion of two samples of HB+HF in LC with 25% HG addition
HB +HF + 25 HG: 85% hydrated Blaue + 15% hydrated Fondu + 25% hydrated gypsum

Both tests show more or less the same values on expansion. The small difference between the 2 tests could be explained by the human error while taking the measurements and difficulty during the sample charging into the LC ring.

The degradation of this blend with and without addition of HG is shown in the next figures (46-47).
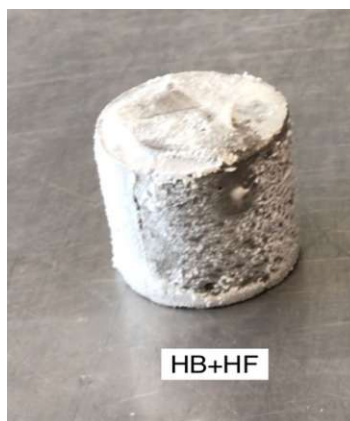
Figure 46 degradation of HB+HF (salt crystallisation)
HB +HF: 85% hydrated Blaue + 15% hydrated Fondu

In figure 46, the blend HB+ HG without HG addition is shown. The sample shows significant amount of salts crystallized on the surface.

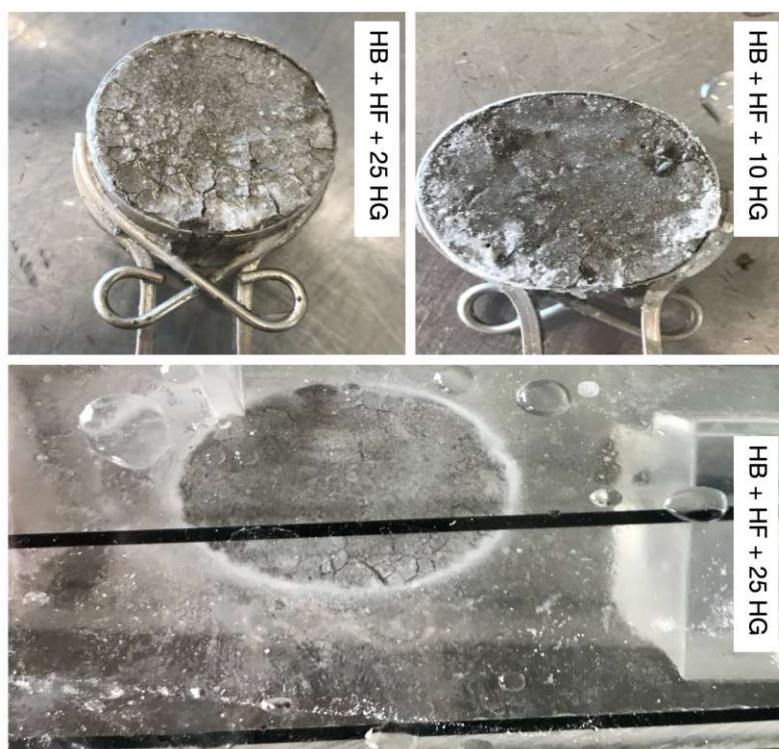The degradation of this blend upon adding HG is shown in figure 47.

Figure 47 degradation of HB+HF+HG
HB +HF + 25 HG: 85% hydrated Blaue + 15% hydrated Fondu + 25% hydrated gypsum

In figure 47 the degradation is shown in form of cracking and spalling. Especially in case of 25% HG addition, the paste cracks to a significant degree.

As already shown, the systems that show significant expansion are HB and the blend HB+HF upon adding 25% HG. Only in these systems the confinement with the Plexiglas frame was applied. For these systems that have high consistency and high expansion, the LC could be considered as a good tool to investigate the expansion due to ISA.

 In all the other systems, no confinement is applied because of the low consistency of the cement paste (as in HF), lack of expansion due to the composition of the cement (HC+ HG). The 1.5 available tolerance between the sample and the Plexiglas frame allows the sample to move freely without any confinement. For these systems the expansion measurement is not

reliable. LC tests for 5, 10% HG addition were also conducted, but not shown here. The results were not reproducible due to the lack of confinement and problems in the setup.

With 50% HG replacement, the consistency of the cement pastes is high as shown by the result of Camber [51]. With such consistency, the samples could be placed more easily in the LC rings without compromising leakage of the cement paste.

4. Conclusion and perspectives

4.1 Conclusion

A range of cements with different aluminate contents were investigated after adding hydrated gypsum, focusing on their potential expansive behaviour. Mortar prisms were made of fresh Fondu cement powder and the expansion after wetting drying cycles was measured. Hydrated cement powders were produced, and gypsum was added to simulate the ISA in recycled cements. The early hydration reactivity after remixing with water was measured with oscillation rheology. The expansion was measured with LC expansion rings. Oedometer with thermal bath setup was tentatively used to measure crystallization pressure in confined space.

The rheological tests showed that the early reactivity of HF was very sensitive to HG addition due to the formation of hydration products (most likely (secondary) ettringite, to confirm this, XRD need to be conducted). Adding HG to HB and to the blended hydrated cement (HB + HF) seemed to delay the further hydration of C_3S and C_2S and fragilized the paste (less strength and less resistance to expansion caused by ettringite formation). The HC showed no change in early reactivity upon HG addition. The confinement in LC worked well for cement pastes with high consistency and high values of expansion (i.e., HB, HB+HF). The blend (HB+HF) showed the highest expansion and deterioration upon addition of HG (consistently with the rheology tests). For HC+ HG (C_3A-free) and HF (low consistency and high degradation), there was no significant expansion. These samples were free to expand in all directions and they were not confined with the Plexiglas frame. The testing time (42 days) of the mortar prisms was very short for a significant ISA-induced expansion to happen. All the prisms with 0% HG showed continuous shrinkage. The addition of HG led to a small initial expansion. The values of expansion were reduced after each weathering cycle. The Oedometer was very sensitive to temperature change and therefore the one-dimensional expansion could not be performed.

4.2 Perspectives

Other (measures) or tests can be done to provide further understanding of the ISA and to relate the expansion measured in LC and the early hydration reactivity in rheological tests to the ettringite formation. These are:

- prolonged testing time for the mortar prisms with higher HG addition
- calorimetry tests to monitor the heat release during the hydration
- XRD (in situ and ex situ) tests to quantify new hydration products (e.g., ettringite) and to monitor the consumption of the existing ones (e.g., C2SH or CH)
- increasing the HG addition in LC (e.g., 50%)

5. Appendix

Six oedometer cells integrated in compressing device were available and used for implementing the oedometer tests. In calibration tests, the oedometer response was tested for different material (e.g., plexiglass, firestone and steel) to test the sensitivity of the oedometer to temperature changes.

Figure 48 shows a sample of Plexiglas tested in the oedometer (dry test). The x-axis shows the testing time in hours and the y-axis shows vertical stress in (kPa).
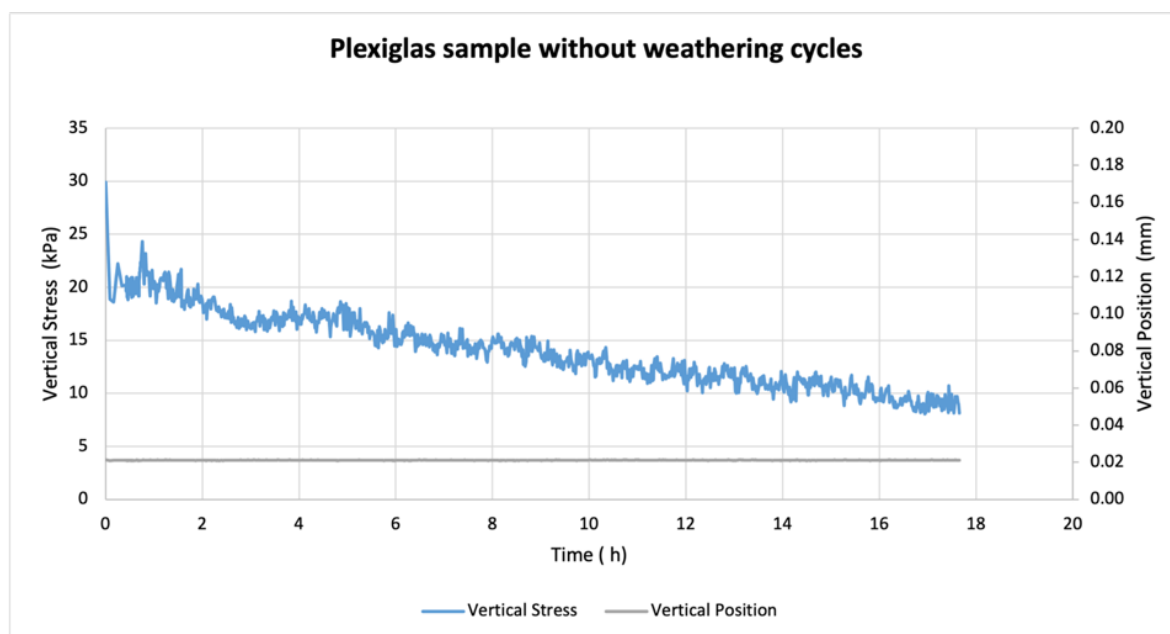

Figure 48 Oedometer calibration test: Plexiglas without weathering cycles

Keeping the sample under constant strain (the same vertical position) results in continuous reduction in the vertical stress (not expected).
In figure 49, the same sample was submerged in water and the test was repeated to test the response of the oedometer.
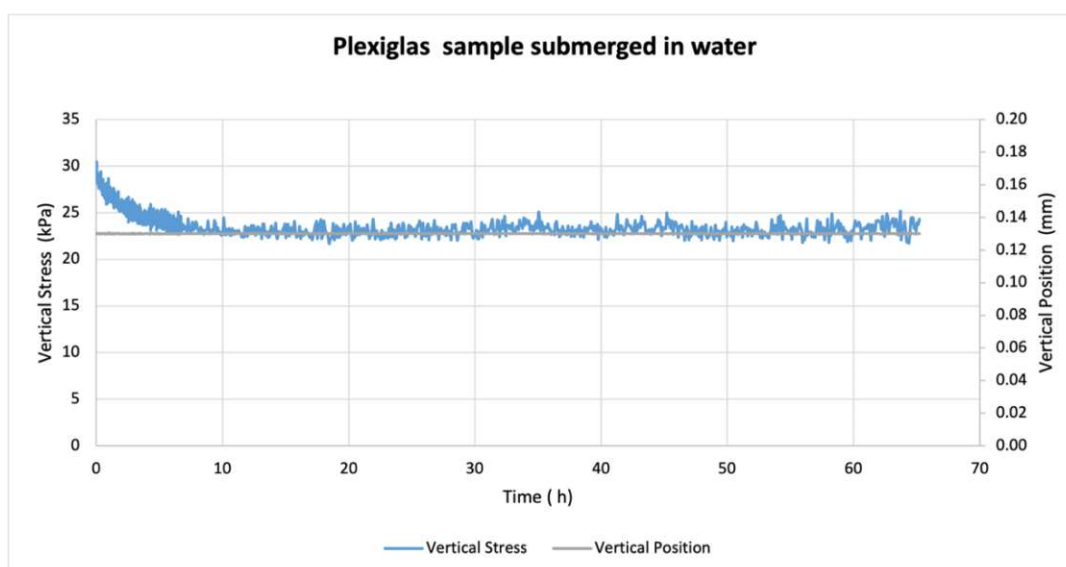

Figure 49 Oedometer calibration test: Plexiglas submerged in water

The submersion condition leads to change in the resulted vertical stress magnitude. The vertical stress is reduced in the first 6 hours reaching a value of about 22.5 kPa. The value stays constant for the rest of the testing time.

From this test it was not known what the reason for the change in the results is. The Plexiglas is not exposed to thermal load (heating cooling cycles) and only submersion in water is not supposed to affect the behavior of this material (because Plexiglas is hydrophobic material).

Another material was chosen to see if the results were changed because of the sensitivity of the oedometer load sensor to water. Firestone sample was tested under constant strain and the resulted vertical stress was measured as plotted in figure 50.
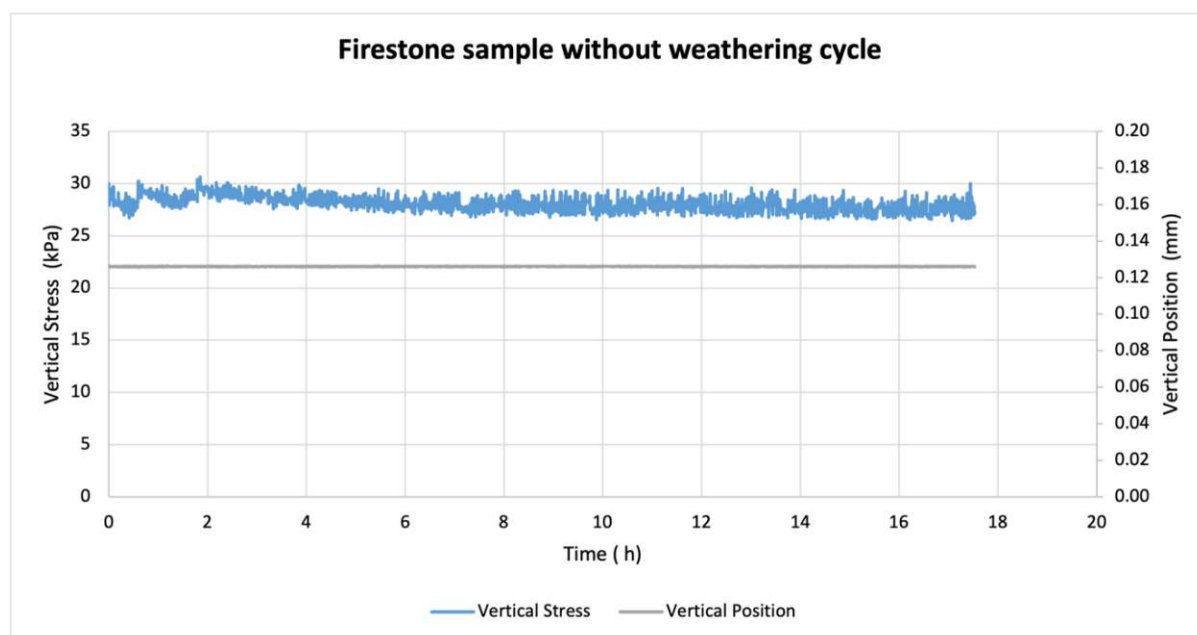

Figure 50 Oedometer calibration test: Firestone without weathering cycles

This test was also implemented in dry condition (no water submersion). There is only insignificant change in the vertical stress. The sample according to this test is considered therefore as stable material, and it does not suffer voluminous change.

To make sure that this result is reproducible, exactly the same test was repeated in another oedometer from the 6 devices available and it is shown in figure 51.

It can be seen from figure 51, that the response of the oedometer devices to the same sample and the same conditions is totally different. This leads to the conclusion that a calibration of the 6 oedometer devices is probably required to get reproducible results. It was not possible to draw a conclusion based on the comparison between the Plexiglas and firestone samples responses to the same test. The variables now are both the materials and the response of the oedometer.
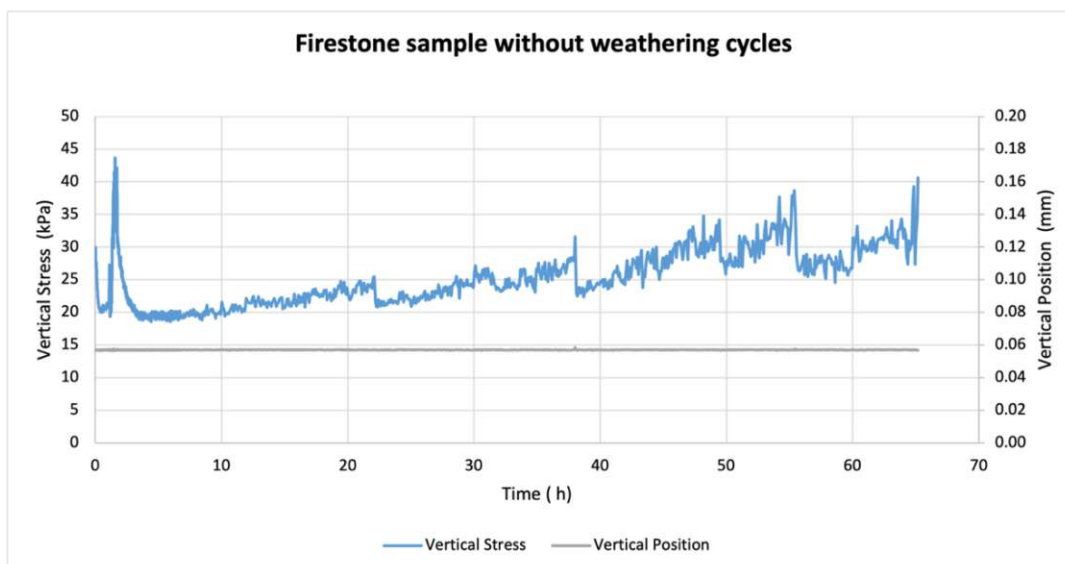
Figure 51 Oedometer calibration test: Firestone without weathering cycles (reproducibility?)

In figure 52, the firestone sample is tested under submersion in water (22 °C).
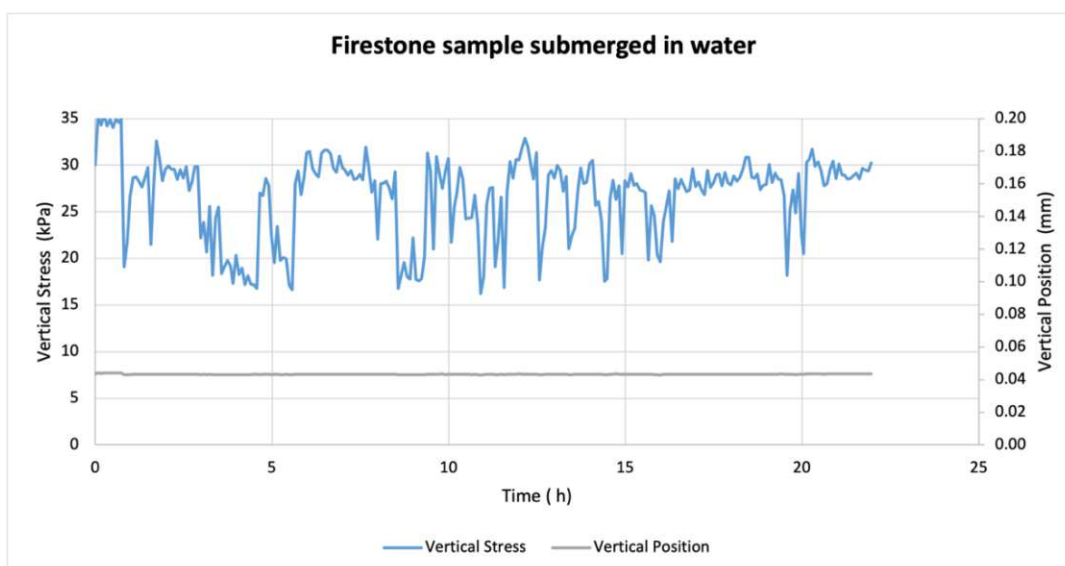

Figure 52 Oedometer calibration test: Firestone submerged in water

The fluctuation in the resulting vertical stress is significant. The water was pumped into the thermal bath and kept at the same temperature during the entire test. The load sensor was also in contact with water and this is probably the reason for the fluctuation in the results.

Steel samples were also tested under the same conditions (no water and no thermal load). Two of these tests are plotted in the next figures (53-54).
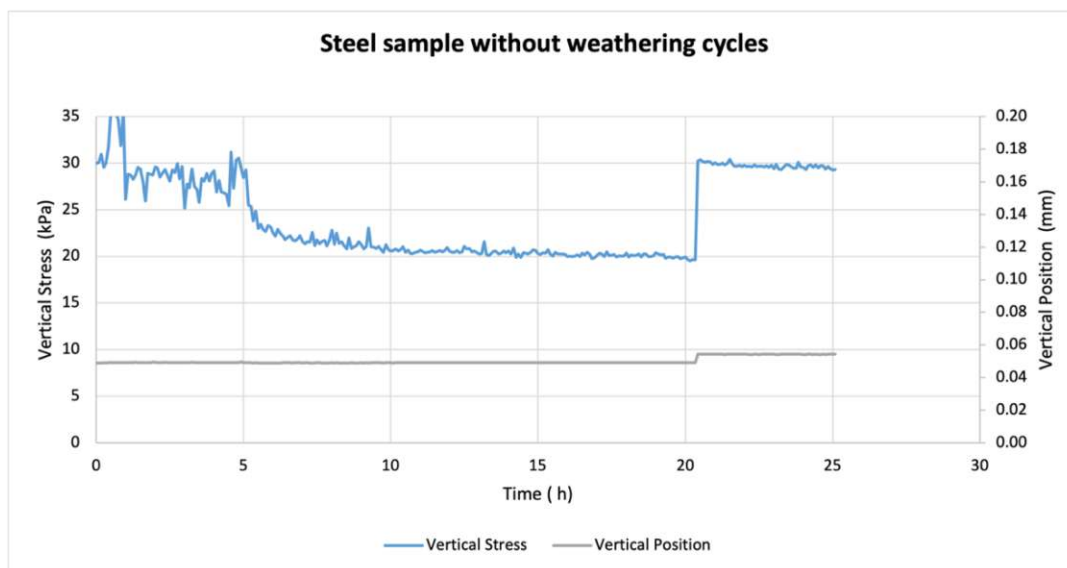
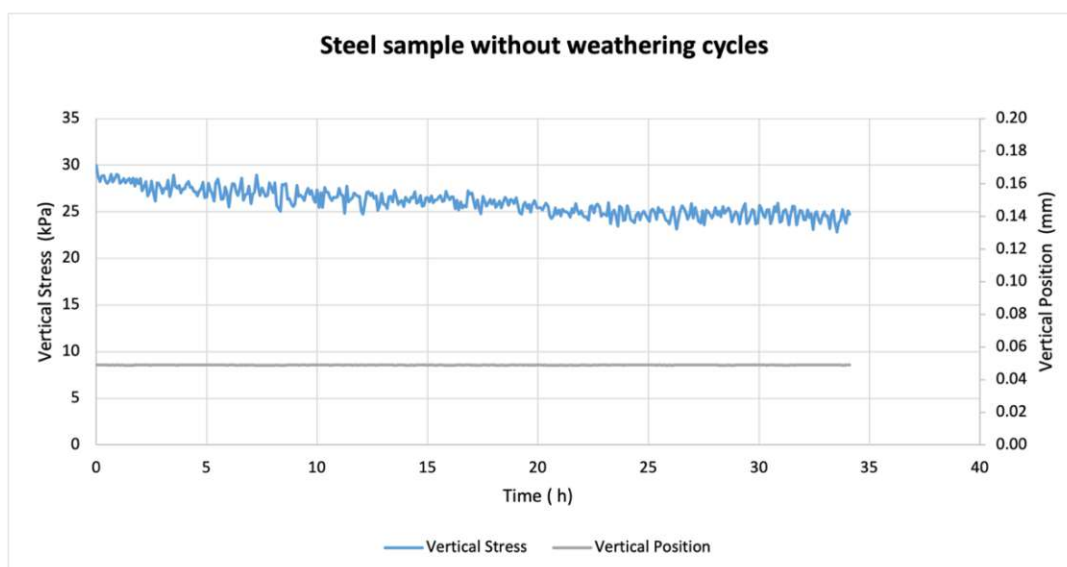*Figure 53 Oedometer calibration test: Steel without weathering cycles*

Figure 54 Oedometer calibration test: Steel without weathering cycles (reproducibility?)

From these two figures the difference in vertical stress for the same material and under the same conditions is shown. The reduction in the vertical stresses in both tests is quite different and therefore the results are each time not reproducible.

The firestone samples were then tested under cooling heating cycles and the results are shown in the next figures (55-56). The vertical stress and water bath temperature are shown on the left y- axis and the vertical position (strain) on the right y-axis.
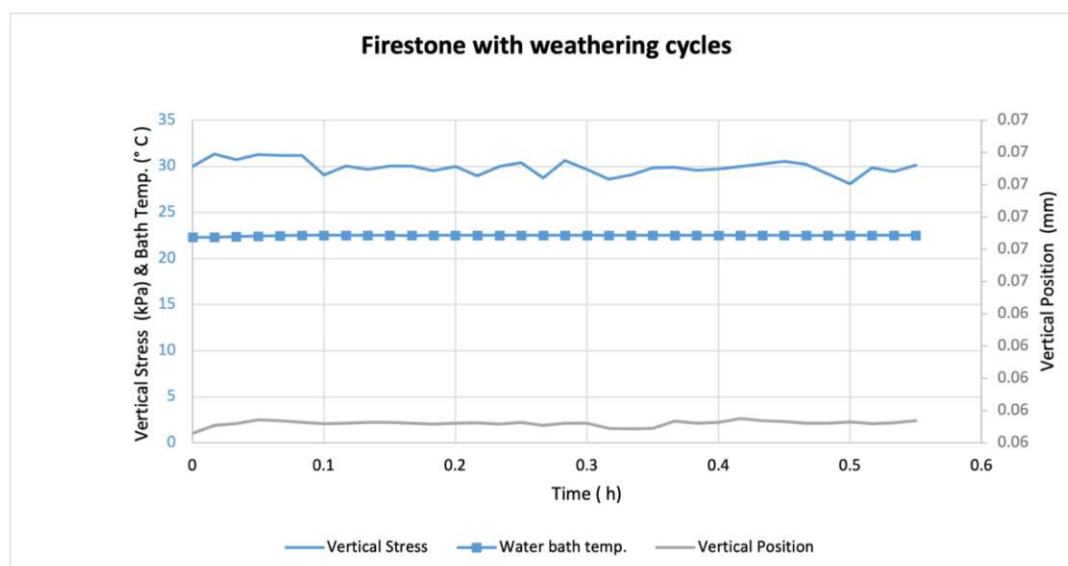
Figure 55 Firestone with weathering cycles

The water bath temperature (Figure 55) was kept at about 22 °C and the strain was fixed after the first few minutes. The vertical stress shows small changes during the testing time.

The test was repeated with raising the temperature gradually from 22°C to 30.5 °C as shown in figure 56.
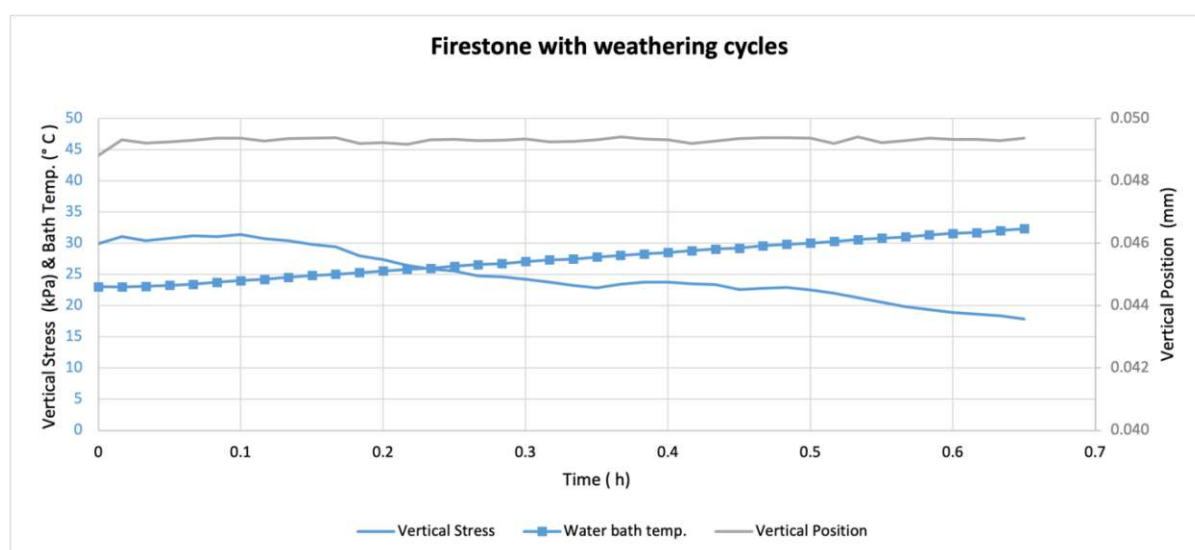

Figure 56 Firestone with weathering cycles (reproducibility?)

The sample shows decrease in stress after 10 minutes from the beginning of the test (about 24°C). This shows that the oedometer sensor is highly sensitive to temperature changes. It was decided to stop the oedometer tests because there were too many variable affecting the reproducibility of the measurements.

The expansion for the mortar prisms of cement Der Blaue (B) is shown in the next figures (57-60).

In figure 57, the expansion is shown for the mortar prisms without hydration gypsum and with 2 w/c ratios (0.5 and 0.65).
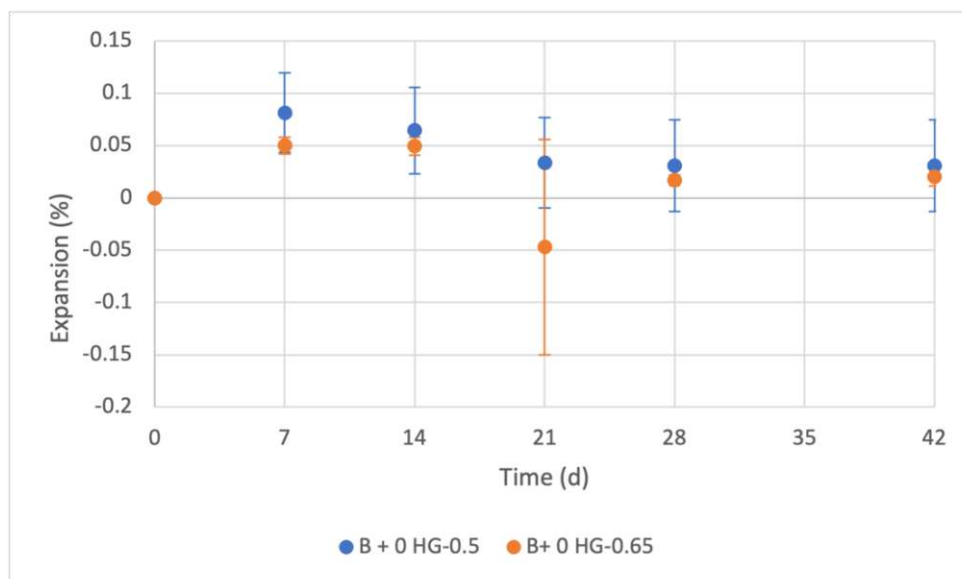
Figure 57 Expansion of the mortar prisms
B + 0 HG-0.5: Blaue+ 0 hydrated gypsum and w/c=0.5,
B + 0 HG-0.65: Blaue + 0 hydrated gypsum and w/c=0.65

The prisms with w/c=0.5 and 0.65 expand in the first cycle (day 7) and then the value of the expansion is reduced in each cycle until the end of the test.

In figure 58, the expansion is shown for the mortar prisms with hydration gypsum (5% HG) and two fineness (coarse and fine HG) and with 2 w/c ratios (0.5 and 0.65).

Figure 58 Expansion of the mortar prisms
B + 5 HG-c-0.5: Blaue + 5 hydrated gypsum, c= coarse gypsum and w/c=0.5,
B + 5 HG-f-0.5: Blaue + 5 hydrated gypsum, fine gypsum and w/c=0.5,
B + 5 HG-c-0.65: Blaue + 5 hydrated gypsum, coarse gypsum and w/c=0.65,
B + 5 HG-f-0.65: Blaue + 5 hydrated gypsum, fine gypsum and w/c=0.65

Expansion happens after the first and 2nd cycles (day 7 and 14) for all the prisms. The sample B + 5 HG-f-0.65 and B + 5 HG-f-0.5 show 0% expansion starting from the third cycle until the end of the test.

In figure 59, the expansion is shown for the mortar prisms with hydration gypsum (10% HG) and two fineness (coarse and fine HG) and with 2 w/c ratios (0.5 and 0.65).
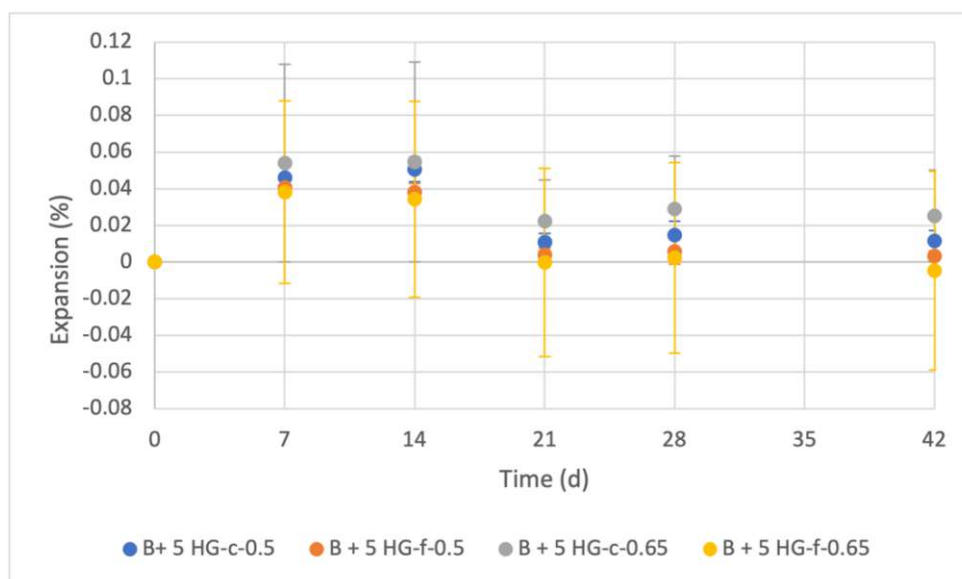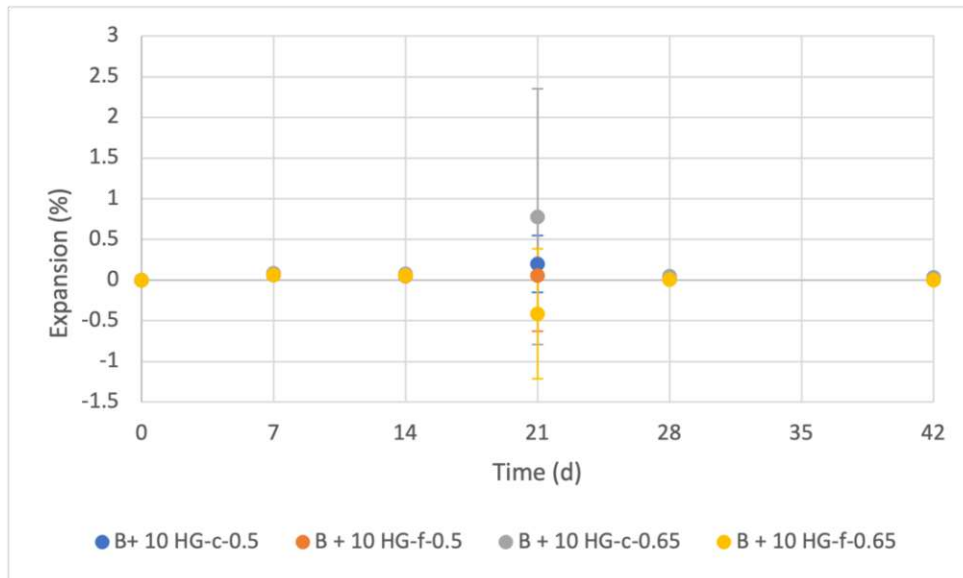
Figure 59 Expansion of the mortar prisms
B + 10 HG-c-0.5: Blaue + 10 hydrated gypsum, c= coarse gypsum and w/c=0.5,
B + 10 HG-f-0.5: Blaue + 10 hydrated gypsum, fine gypsum and w/c=0.5,
B + 10 HG-c-0.65: Blaue + 10 hydrated gypsum, coarse gypsum and w/c=0.65,
B + 10 HG-f-0.65: Blaue + 10 hydrated gypsum, fine gypsum and w/c=0.65

Due to an error in measuring 1 of the 3 replicates, neither shrinkage nor expansion could be shown except in the 3rd cycle (day 21).

The figure is zoomed in below to enable plotting all of the samples
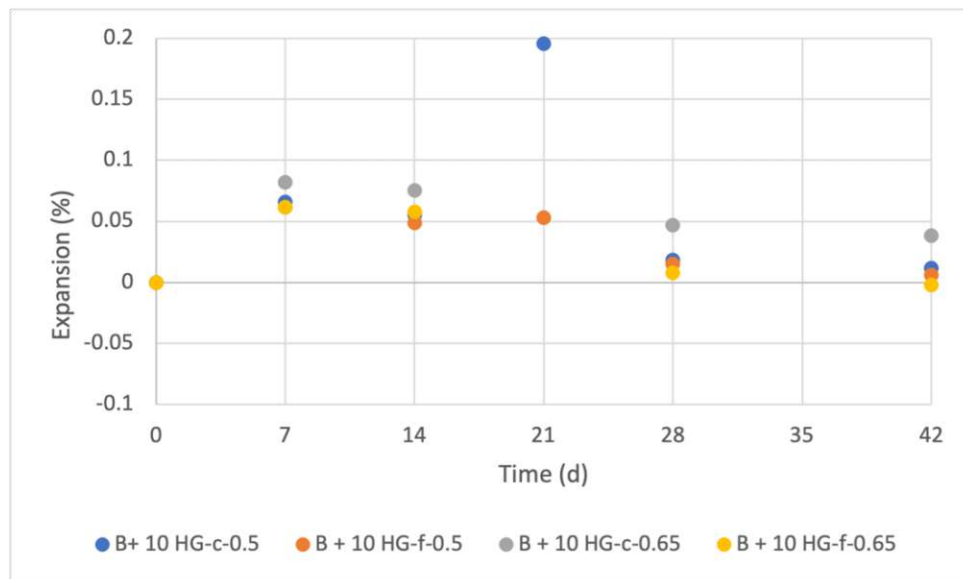
Figure 60 Expansion of the mortar prisms (zoomed in)
B + 10 HG-c-0.5: Blaue + 10 hydrated gypsum, c= coarse gypsum and w/c=0.5,
B + 10 HG-f-0.5: Blaue + 10 hydrated gypsum, fine gypsum and w/c=0.5,
B + 10 HG-c-0.65: Blaue + 10 hydrated gypsum, coarse gypsum and w/c=0.65,
B + 10 HG-f-0.65: Blaue + 10 hydrated gypsum, fine gypsum and w/c=0.65

It can be seen from figure 60 that actually all the prisms expand in all of the cycles. The value on expansion decrease after each cycle until the end of the test.

6. Literatures

1. Liberto, T., *Physico-chemical study of calcite colloidal suspensions: from macroscopic rheology to microscopic interaction*. 2018, Université de Lyon.
2. Monteiro, P.J.M. and K.E. Kurtis, *Time to failure for concrete exposed to severe sulfate attack.* Cement and Concrete Research, 2003. **33**(7): p. 987-993.
3. Yin, G.-J., et al., *An integrated macro-microscopic model for concrete deterioration under external sulfate attack.* Engineering Fracture Mechanics, 2020. **240**: p. 107345.
4. Zhao, G., et al., *Degradation of cast-in-situ concrete subjected to sulphate-chloride combined attack.* Construction and Building Materials, 2020. **241**: p. 117995.
5. Liao, K.-X., et al., *Modeling constitutive relationship of sulfate-attacked concrete.* Construction and Building Materials, 2020. **260**: p. 119902.
6. Neville, A., *The confused world of sulfate attack on concrete.* Cement and Concrete Research, 2004. **34**(8): p. 1275-1296.
7. Colman, C., et al., *Internal sulfate attack in mortars containing contaminated fine recycled concrete aggregates.* Construction and Building Materials, 2021. **272**: p. 121851.
8. Zhang, H., T. Ji, and H. Liu, *Performance evolution of recycled aggregate concrete (RAC) exposed to external sulfate attacks under full-soaking and dry-wet cycling conditions.* Construction and Building Materials, 2020. **248**: p. 118675.
9. Scherer, G.W., *Crystallization in pores.* Cement and Concrete Research, 1999. **29**(8): p. 1347-1358.
10. Zhang, M., et al., *Study on the expansion of concrete under attack of sulfate and sulfate–chloride ions.* Construction and Building Materials, 2013. **39**: p. 26-32.
11. Al-Attar, T.S., A.M. Al-Khateeb, and A.H. Bachai, *Behavior of High Performance Concrete Exposed to Internal Sulfate Attack (Gypsum-Contaminated Aggregate).* Earth & Sp, 2006: p. 1-6.
12. Meng, C., et al., *Experimental research on durability of high-performance synthetic fibers reinforced concrete: Resistance to sulfate attack and freezing-thawing.* Construction and Building Materials, 2020. **262**: p. 120055.
13. Wang, K., et al., *Influence of dry-wet ratio on properties and microstructure of concrete under sulfate attack.* Construction and Building Materials, 2020. **263**: p. 120635.
14. Mindess, S., *6 - Resistance of Concrete to Destructive Agencies*, in *Lea's Chemistry of Cement and Concrete (Fifth Edition)*, P.C. Hewlett and M. Liska, Editors. 2019, Butterworth-Heinemann. p. 251-283.
15. Scherer, G.W., *Stress from crystallization of salt.* Cement and Concrete Research, 2004. **34**(9): p. 1613-1624.
16. Ideker, J.H., et al., *12 - Calcium Aluminate Cements*, in *Lea's Chemistry of Cement and Concrete (Fifth Edition)*, P.C. Hewlett and M. Liska, Editors. 2019, Butterworth-Heinemann. p. 537-584.
17. Diamond, S., *Delayed ettringite formation — Processes and problems.* Cement and Concrete Composites, 1996. **18**(3): p. 205-215.
18. Benedix, R., *Bauchemie für das Bachelor-Studium*. 2014: Springer.
19. Oliveira, I., S.H.P. Cavalaro, and A. Aguado, *New kinetic model to quantify the internal sulfate attack in concrete.* Cement and Concrete Research, 2013. **43**: p. 95-104.
20. Zou, D., et al., *Experimental and numerical study of the effects of solution concentration and temperature on concrete under external sulfate attack.* Cement and Concrete Research, 2021. **139**: p. 106284.
21. Mehta, P.K., *Scanning electron micrographic studies of ettringite formation.* Cement and Concrete Research, 1976. **6**(2): p. 169-182.
22. Mehta, P.K., *Mechanism of sulfate attack on portland cement concrete — Another look.* Cement and Concrete Research, 1983. **13**(3): p. 401-406.

23. Taylor, H.F.W., C. Famy, and K.L. Scrivener, *Delayed ettringite formation.* Cement and Concrete Research, 2001. **31**(5): p. 683-693.

24. Ouyang, C., A. Nanni, and W.F. Chang, *Internal and external sources of sulfate ions in portland cement mortar: two types of chemical attack.* Cement and Concrete Research, 1988. **18**(5): p. 699-709.

25. Harrisson, A.M., *4 - Constitution and Specification of Portland Cement*, in *Lea's Chemistry of Cement and Concrete (Fifth Edition)*, P.C. Hewlett and M. Liska, Editors. 2019, Butterworth-Heinemann. p. 87-155.

26. Herfort, D. and D.E. Macphee, *3 - Components in Portland Cement Clinker and Their Phase Relationships*, in *Lea's Chemistry of Cement and Concrete (Fifth Edition)*, P.C. Hewlett and M. Liska, Editors. 2019, Butterworth-Heinemann. p. 57-86.

27. Thomas, J.J. and H.M. Jennings, *Materials of cement science primer: The science of concrete*. 2009.

28. Odler, I. and M. Gasser, *Mechanism of sulfate expansion in hydrated Portland cement.* Journal of the American Ceramic Society, 1988. **71**(11): p. 1015-1020.

29. theconstructor.org. Available from: https://test.theconstructor.org/concrete/steam-curing-concrete-methods-advantages/38837/.

30. Paine, K.A., *7 - Physicochemical and Mechanical Properties of Portland Cements☆*, in *Lea's Chemistry of Cement and Concrete (Fifth Edition)*, P.C. Hewlett and M. Liska, Editors. 2019, Butterworth-Heinemann. p. 285-339.

31. Schmidt, T., et al., *A thermodynamic and experimental study of the conditions of thaumasite formation.* Cement and Concrete Research, 2008. **38**(3): p. 337-349.

32. Sims, I., J. Lay, and J. Ferrari, *15 - Concrete Aggregates*, in *Lea's Chemistry of Cement and Concrete (Fifth Edition)*, P.C. Hewlett and M. Liska, Editors. 2019, Butterworth-Heinemann. p. 699-778.

33. Ting, M.Z.Y., et al., *Deterioration of marine concrete exposed to wetting-drying action.* Journal of Cleaner Production, 2021. **278**: p. 123383.

34. Yu, X.-t., et al., *Behavior of mortar exposed to different exposure conditions of sulfate attack.* Ocean Engineering, 2018. **157**: p. 1-12.

35. Gao, J., et al., *Durability of concrete exposed to sulfate attack under flexural loading and drying–wetting cycles.* Construction and Building Materials, 2013. **39**: p. 33-38.

36. Li, J., et al., *Experimental and numerical investigation of cast-in-situ concrete under external sulfate attack and drying-wetting cycles.* Construction and Building Materials, 2020. **249**: p. 118789.

37. Xie, F., et al., *Experimental study on performance of cast-in-situ recycled aggregate concrete under different sulfate attack exposures.* Construction and Building Materials, 2020. **253**: p. 119144.

38. Tang, J., et al., *Development of properties and microstructure of concrete with coral reef sand under sulphate attack and drying-wetting cycles.* Construction and Building Materials, 2018. **165**: p. 647-654.

39. Famy, C., et al., *Influence of the storage conditions on the dimensional changes of heat-cured mortars.* Cement and Concrete Research, 2001. **31**(5): p. 795-803.

40. Oikonomou, N.D., *Recycled concrete aggregates.* Cement and Concrete Composites, 2005. **27**(2): p. 315-318.

41. Zhao, G., et al., *Degradation mechanisms of cast-in-situ concrete subjected to internal-external combined sulfate attack.* Construction and Building Materials, 2020. **248**: p. 118683.

42. ÖNORM EN 196-1, *Methods of testing cement - Part 1: Determination of strength*. 2016.

43. Mezger, T.G., *Applied rheology: with Joe flow on rheology road*. 2015: Anton Paar.

44. ÖNORM EN 196-3, *Determination of setting times and soundness*, in 2017.

45. geotesting.org. Available from: http://www.geotesting.org/geotest/standard-oedometer-test.

46. geoengineer.org. Available from: https://www.geoengineer.org/education/laboratory-testing/soil-consolidation.

47.   del Strother, P., *2 - Manufacture of Portland Cement*, in *Lea's Chemistry of Cement and Concrete (Fifth Edition)*, P.C. Hewlett and M. Liska, Editors. 2019, Butterworth-Heinemann. p. 31-56.
48.   Lafarge;. Available from: https://www.lafarge.at/zement/sackzement/der-contragress-cem-i-425-n.
49.   Müllauer, W., *Mechanismen des Sulfatangriffs auf Beton–Phasenneubildungen und Expansionsdrücke in Mörteln unter Na2SO4 Belastung*. 2013, Technische Universität München.
50.   Bollmann, K., *Ettringitbildung in nicht wärmebehandelten Betonen.* 2000.
51.   Camber, R., *Untersuchungen zu Treiberscheinungen in Beton ausgelöst durch rezyklierte Gesteinskörnung*. Investigations on expansion phenomena in concrete caused by recycled aggregates. 2021, Wien: Wien. 78 Seiten.
52.   Liberto, T., M. Bellotto, and A. Robisson, *Small oscillatory rheology and cementitious particle interactions.* Cement and Concrete Research, 2022. **157**: p. 106790.
53.   Shirani, S., et al., *Calcium aluminate cement conversion analysed by ptychographic nanotomography.* Cement and Concrete Research, 2020. **137**: p. 106201.
54.   Nehring, J., et al., *Acceleration of OPC by CAC in binary and ternary systems: The role of pore solution chemistry.* Cement and Concrete Research, 2018. **107**: p. 264-274.
55.   Evju, C. and S. Hansen, *Expansive properties of ettringite in a mixture of calcium aluminate cement, Portland cement and β-calcium sulfate hemihydrate.* Cement and Concrete Research, 2001. **31**(2): p. 257-261.